XBeach WTI2017, revision 4872

quality status report

Revision: 4872

November 3, 2015

XBeach WTI2017, revision 4872

Published and printed by:

Deltares
Rotterdamseweg 185
p.o. box 177
2600 MH Delft
The Netherlands

telephone: +31 88 335 85 85
fax: +31 88 335 85 82
e-mail: info@deltares.nl
www: http://www.deltares.nl

For support contact:

telephone: +31 88 335 85 55
fax: +31 88 335 81 11
e-mail: xbeach@deltares.nl
www: http://www.xbeach.org/

Contents

Chapter 1

Introduction

For the WTI2017 project, one of the deliverables is a new version of the XBeach model, intended for use as an advanced dune safety assessment model. This report describes the requirements for a 1 dimensional advanced dune safety assessment model and tries to show that XBeach meets those requirements. The latter is done by comparing the model results to measurements, either taken during laboratory experiments or in the field.

Chapter 2

Requirements for advanced dune safety assessment

An advanced dune safety assessment is performed when a detailed assessment is considered unsuitable for a certain location or stretch of dune coast. In general, the morphological behaviour at those locations is significantly influenced by physical processes that are lacking in the detailed assessment model (a 1-dimensional profile model), hence the need for a more in-depth advanced assessment. This is the case for approximately 40% of the dutch coastline. The most common causes are listed below:

- **Flat profile slopes** Very flat beach and foreshore slopes are often gentler than the resulting profile of the detailed safety assessment, so no dune erosion is predicted. However, in practice the presence of long waves does cause dune erosion.
- **Irregular profiles** Profiles containing pronounced irregular features like banks or gullies present a problem for the detailed safety assessment model, which imposes a prescribed shape on the final profile.
- **Hybrid sea defenses** These sea defenses consist partly of sand and partly of a hard structure. (for instance sea walls, dune (foot) revetments, dikes with dunes in front).
- **Hard objects** In particular at coastal cities there are often hard objects present on or in front of the sandy sea defense, while not functionally being part of the sea defense. These objects can however have an influence on the morphological behaviour of the sandy sea defense during storm conditions.
- **Time varying storm surge** At locations with a relatively small first dune row, that might fail during design conditions, time varying storm conditions become essential for a proper assessment.

  The moment of failure in view of the total storm influences the probability of inundation of the dune area or hinterland.

In the table below, the functional requirements to the WTI2017 version of XBeach are summarized and translated into physical processes the model should be able to resolve successfully.

Table 2.1: Translation of functional requirements into physical processes

Functional requirement	Physical process
Dune erosion	hydrodynamics, morphodynamics
Gentle slopes	long waves
Irregular profile shapes (banks & gullies)	process based model (no prescribed final profile)
Structures & objects	hard layers, scour holes
Realistic storm forcing	time varying storm surge & wave forcing

The WTI2017 version of XBeach is supposed to be a solution to the above mentioned problems. To be able to show that XBeach is capable of doing so, the model results will be compared to large and small scale laboratory measurements and field data. Before doing this, the required functionalities have to be translated in to measurable physical aspects, on which the comparison will be made. This is shown in the table below, including the availability of measurements for comparison on each aspect.

Table 2.2: Overview of relevant physical processes in dune safety assessment

Physical aspect	Experimental (small scale)	Experimental (large scale)	Field observations
Hydrodynamics			
Water levels		✓	
Wave heights		✓	
Velocities	✓	✓	
Morphology			
Erosion volume	✓	✓	✓
Erosion profile	✓	✓	✓
Sediment concentration		✓	
Hard layers/structures	✓	✓	✓
Scour holes		✓	

2.1 Skill comparison between releases

In the table below, the Brier Skill Scores for the final profile of several different tests are summarized. The scores at the time of the Easter release of XBeach (April 6th, 2012) are compared to the scores of the current WTI2017 release, to show the skill development between those two releases. Some of the tests have been added to the skillbed after the Easter release, so the BSS of the Easter release fot those tests is not available, which is indicated by a score of 0 in the table.

Table 2.3: Brier Skill Score comparison between WTI2017 and previous Easter release.

Test name	BSS Easter release	Current BSS	Difference
Deltaflume M1263 III Test-1	0.89	0.91	0.02
Test-2	0.95	0.96	0.01
Test-3	0.87	0.90	0.03

Test-4	0.64	0.65	0.01
Test-5	0.98	0.98	0.00
Deltaflume2006 T01	0.95	0.94	-0.01
T02	0.94	0.93	-0.01
T03	0.96	0.96	0.00
T04	0.80	0.80	0.00
DP01	0.86	0.85	-0.01
DP02	0.40	0.39	-0.01
DeltaflumeLIP11D 2E	0.84	0.82	-0.02
GWK86 T01		0.95	
T02		0.27	
T03		0.65	
T04		-0.73	
T05		-3.01	
T06		0.80	
GWK98 A9		-1.17	
B2		0.81	
C2		0.07	
F1		0.38	
H2		-0.43	
Scheldtflume H4265 T01		0.86	
T02		0.83	
T02a		0.87	
T03		0.90	
T11		0.65	
T12		0.74	
T13		0.81	
Scheldtflume M1819 I T01		0.72	
T02		0.72	
T03		0.74	
T04		0.67	
T05		0.68	
T06		0.66	
T07		0.66	
T08		0.30	
T09		0.29	
T10		0.72	
T11		0.79	
T12		0.15	
T13		0.64	
T14		0.65	
T21		0.63	
T22		0.39	
T23		0.62	
T24		0.55	
T25		0.36	
T26		0.53	
T27		0.71	
T28		0.89	
T29		0.66	

Deltaflume M1263 I AT33	0.88	0.88	-0.00
AT47	0.59	0.59	-0.00
AT61	0.70	0.66	-0.04
AT71	0.74	0.65	-0.09
AT91	0.71	0.68	-0.03
AT95	0.27	0.36	0.09
BT13	0.73	0.70	-0.03
BT15	0.71	0.66	-0.05
BT17	0.61	0.61	0.00
BT23	0.73	0.72	-0.01
BT25	0.83	0.81	-0.02
BT27	0.69	0.69	0.00
BT45	0.68	0.61	-0.07
BT62	0.61	0.60	-0.01
BT72	0.68	0.66	-0.02
BT92	0.61	0.59	-0.02
BT96	0.78	0.79	0.01
CT14	0.69	0.68	-0.01
CT16	0.75	0.73	-0.02
CT18	0.42	0.49	0.07
CT24	0.86	0.83	-0.03
CT26	0.78	0.79	0.01
CT28	-0.17	-0.08	0.09
CT46	-1.53	-1.52	0.01
CT63	0.81	0.79	-0.02
CT73	0.85	0.82	-0.03
CT93	0.71	0.69	-0.02
CT97	0.85	0.85	-0.00
DT34	0.85	0.85	-0.00
DT48	0.64	0.63	-0.01
DT64	0.70	0.68	-0.02
DT74	0.91	0.90	-0.01
DT94	0.70	0.67	-0.03
DT98	-0.67	-0.57	0.10
Deltaflume M1263 II 101	0.56	0.62	0.06
105	0.24	0.39	0.15
111	0.54	0.63	0.09
115	0.07	0.27	0.20
121	0.93	0.93	-0.00
122	0.84	0.86	0.02
123	0.79	0.73	-0.06
124	0.54	0.50	-0.04
125	-0.33	-0.36	-0.03
126	0.72	0.74	0.02
127	0.55	0.47	-0.08
128	0.41	0.42	0.01
1976 storm surge raai3400	0.72	0.57	-0.15
raai568	0.65	0.71	0.06
raai6050	0.96	0.94	-0.02
Deltaflume H4731 T11		-29.90	

T12		0.17	
T14		0.68	
DeltaflumeH298 T1	0.58	0.75	0.17
T2	0.54	0.77	0.23
T3	0.79	0.92	0.13
Deltaflume M1797 T01		0.87	
T02		0.95	
Scheldtflume M1819 III T01		0.05	
T02		0.89	
T03		0.91	
T04		0.75	

Chapter 3

1D Hydrodynamics

The hydrodynamics form the basis for the morphodynamic behaviour. In this chapter the hydrodynamic results of XBeach are discussed. All tests are run without the morphological module and the analysis is focused on the wave propagation and transformation computed by XBeach.

First, two analytical solutions are reproduced by XBeach. Subsequently, a laboratory experiment is discussed.

3.1 Long wave propagation

The purpose of the this test is to check if the NSWE numerical scheme is not too dissipative and that it does not create large errors in propagation speed.

A long wave with a small amplitude of $0.01m$ and period of $80s$ was sent into a domain of $5m$ depth, grid size of $5m$ and a length of $1km$. At the end, a fully reflecting wall is imposed. The wave length in this case should be $\sqrt{g \cdot d} \cdot T = \sqrt{9.81 \cdot 5} \cdot 80 = 560m$. The velocity amplitude should be $\sqrt{g/h} \cdot A = \sqrt{9.81/5} \cdot 0.01 = 0.014m$. After the wave has reached the wall, a standing wave with double amplitude should be created.

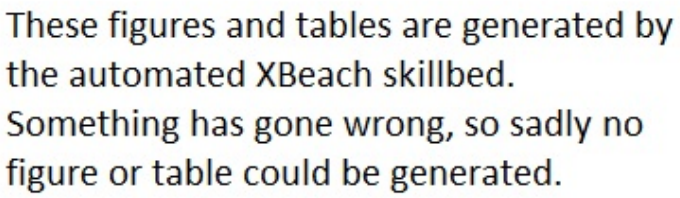

Figure 3.1: Water levels and velocities from the start of the experiment until the wave just reaches the end of the flume

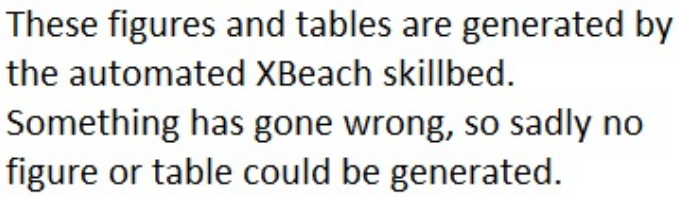

Figure 3.2: Snapshots of water levels and velocities showing a standing wave pattern

3.2 1D wave runup (analytical solution)

The purpose of this test is to check the ability of the model to represent runup and rundown of non-breaking long waves. To that end, a comparison was made with the analytical solution of the NSWE by Carrier and Greenspan (1958), which describes the motion of harmonic, non-breaking long waves on a plane sloping beach without friction.

A free long wave with a wave period of 32 seconds and wave amplitude of half the wave breaking amplitude ($a_{in} = 0.5 \cdot a_{br}$) propagates over a beach with constant slope equal to $1/25$. The wave breaking amplitude is computed as $a_{br} = 1/\sqrt{128} \cdot \pi^3 \cdot s^{2.5} \cdot T^{2.5} \cdot g^{1.25} \cdot h_0^{-0.25} = 0.0307m$, where s is the beach slope, T is the wave period and h_0 is the still water depth at the seaward

boundary. The grid is non uniform and consists of 160 grid points. The grid size Δx is decreasing in shoreward direction and is proportional to the (free) long wave celerity ($\sqrt{g \cdot h}$). The minimum grid size in shallow water was set at $\Delta x = 0.1m$.

To compare XBeach output to the analytical solution of Carrier and Greenspan (1958), the first are non-dimensionalized with the beach slope s, the acceleration of gravity g, the wave period T, a horizontal length scale L_x and the vertical excursion of the swash motion A. The horizontal length scale L_x is related to the wave period via $T = \sqrt{L_x/g \cdot s}$ and the vertical excursion of the swash motion A is expressed as: $A = a_{in} \cdot \pi/\sqrt{0.125 \cdot s \cdot T \cdot \sqrt{g/h_0}}$

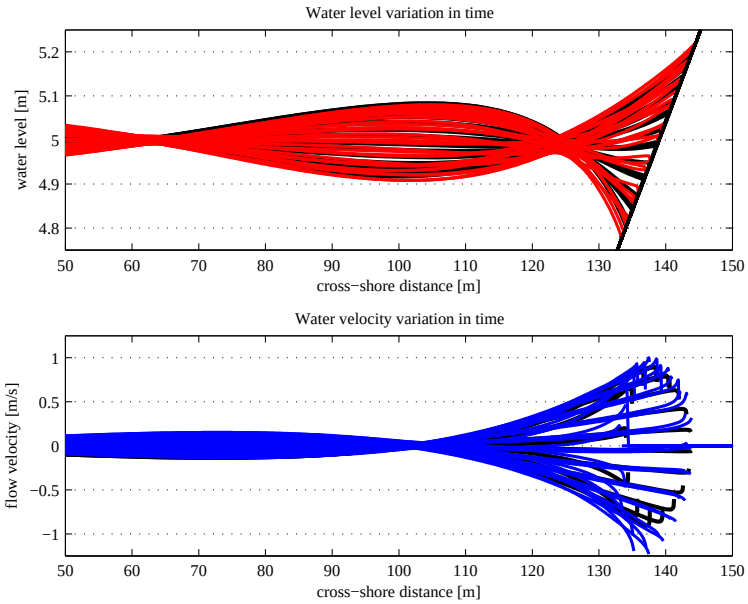

Figure 3.3: Snapshots of water level and velocity

3.3 High- and low-frequency wave transformation

Boers (1996) performed experiments with irregular waves in the physical wave flume at Delft University of Technology with a length of 40 meters and a width of 0.8 m. The flume is equipped with a hydraulically driven, piston type wave generator with second-order wave generation and Active Reflection Compensation. Boers ran waves over a concrete bar-trough beach, which was modelled after the Delta Flume experiments. He ran three different irregular wave conditions, but in this report we will focus on case 1C, a Jonswap spectrum with $H_{m,0} =$ 0.1m and $T_p = 3.3$s. The surface elevation was measured in 70 locations shown in Figure 3.4.

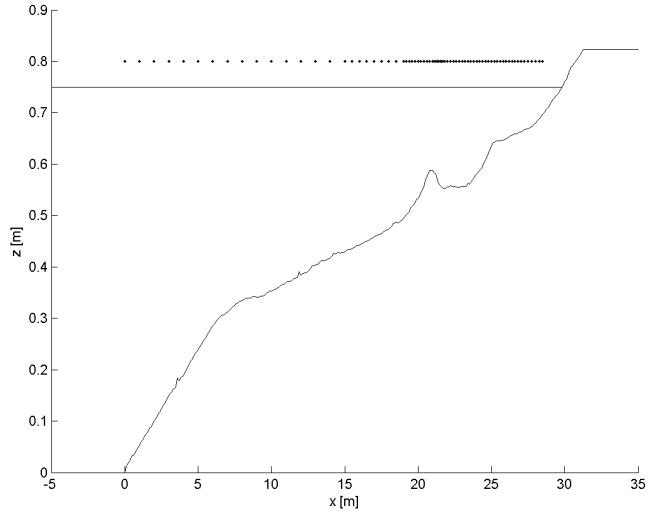

Figure 3.4: Locations of surface eleveation measurements

The comparison between the model and the data for the wave height transformation of the short waves and the long waves (defined as waves with a frequency greater than $f_p/2$ and less than $f_p/2$, respectively) is shown in Figure 3.5.

The red dashed line and triangles indicate the short wave height transformation. The blue line and circles indicate the mean (steady) set-up. The dotted red line and upside-down traiangles indicate the total (incoming and reflected) low frequency wave.

The observational data is separated into incoming and reflected long wave components using an array of wave gauges (Bakkenes, 2002) and the numerical data has been separated into two components using co-located surface elevation and velocity information.

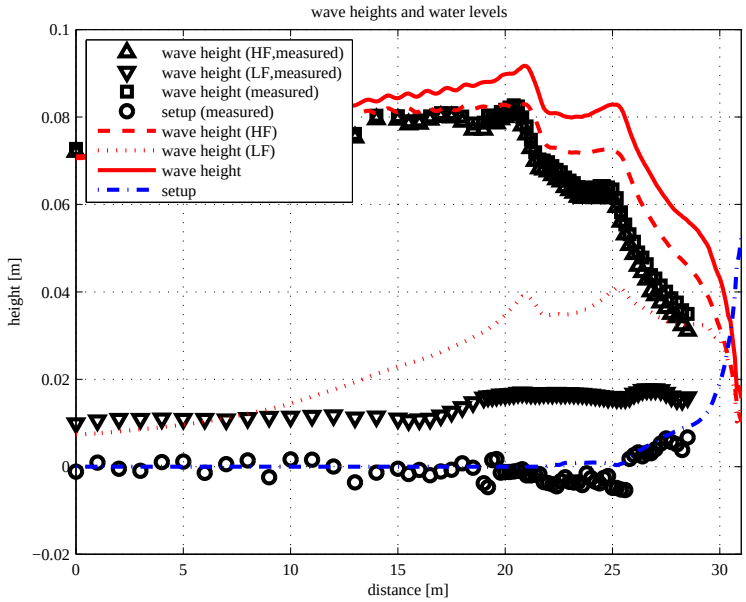

Figure 3.5: Wave height transformations during Boers 1C experiment

Chapter 4

Dune erosion

In this chapter, the performance of XBeach is compared to results obtained from physical model tests performed in a variety of laboratory facilities and field measurements. Many of those tests are part of fundamental research to dune erosion and other morphological processes. Research took place on different scales, mainly depending on the size of the facility used. The chapter separately discusses small scale laboratory tests (with a depth scale factor n_d between 85 and 15), large scale laboratory tests (n_d between 6 and 2, approaching prototype) and field measurements.

As described in the previous chapter, the relevant skill parameters for accurately predicting dune erosion are the post-storm cross-shore profile, the total eroded volume and the sediment concentration near the water line. For all scales mentioned above, an example will be described in more detail, after which an overview of the performance of all available tests will be presented.

4.1 Large scale laboratory tests

4.1.1 M1797: Delta Flume 1981

In 1981, Delta Flume experiments were performed to gain insight in the effect of a dune revetment on the morphological behaviour of the dune. The profile in question is based on a stretch of coast called the Noorderstrand at Schouwen, the Netherlands(Vellinga, 1981a). Two large scale experiments (depth scale of 2) were performed, one with and one without dune revetment. The latter is depicted in Figure 4.1.

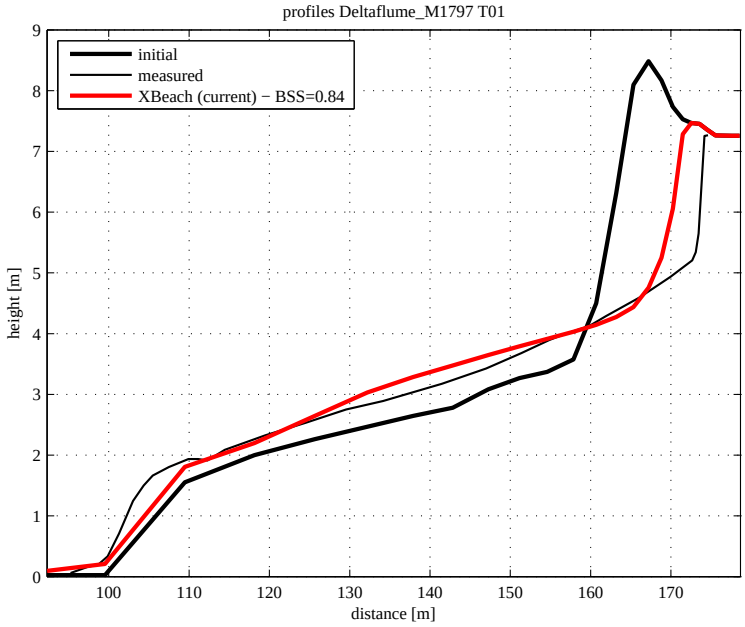

Figure 4.1: Final profile of test T01

4.1.2 M1263 III: Delta Flume 1980-1981

As a continuation of parts I and II of the M1263 experiment series, large scale tests (depth scales between 1 and 5) were performed in the Delta Flume(Vellinga, 1984), with the goal of verifying the relations found at smaller scales. The test result are shown in Figure 4.2 to Figure 4.6.

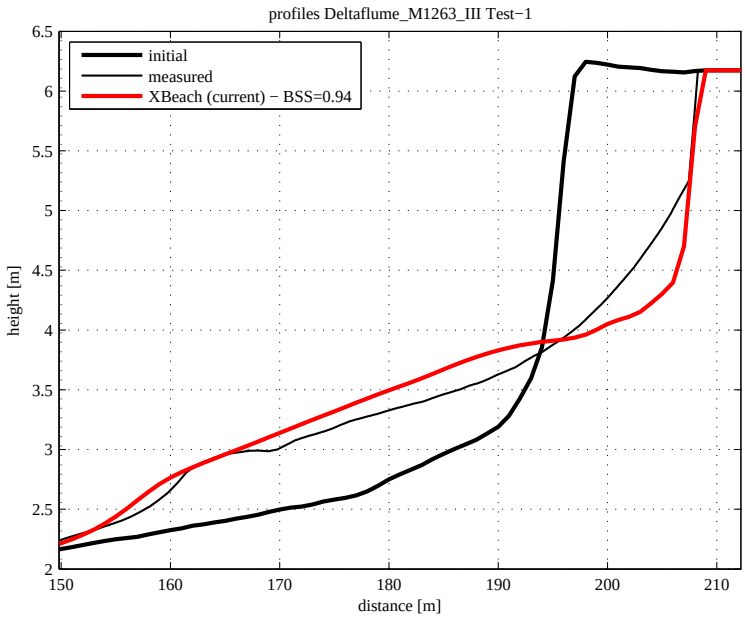

Figure 4.2: Final profile of test 1

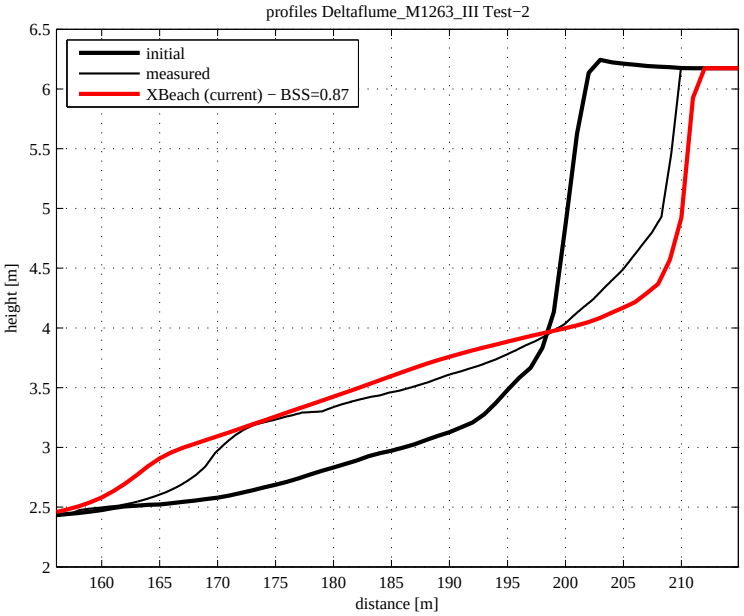

Figure 4.3: Final profile of test 2

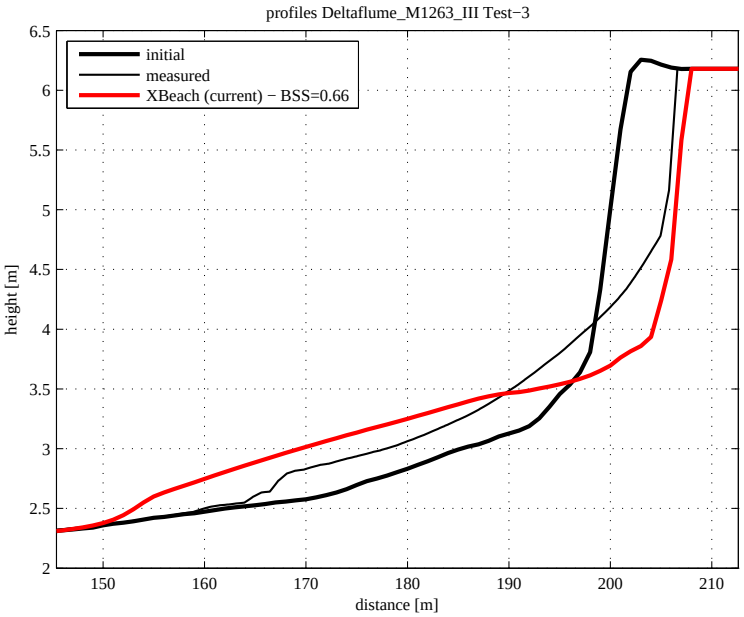

Figure 4.4: Final profile of test 3

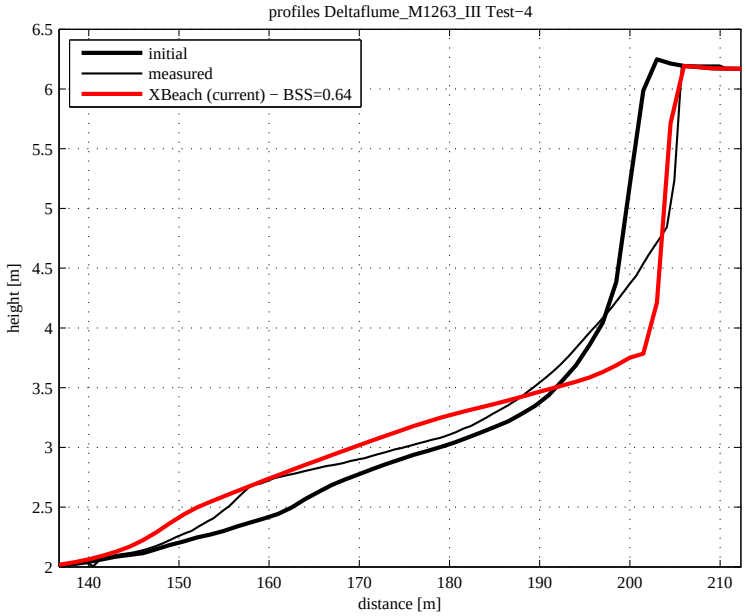

Figure 4.5: Final profile of test 4

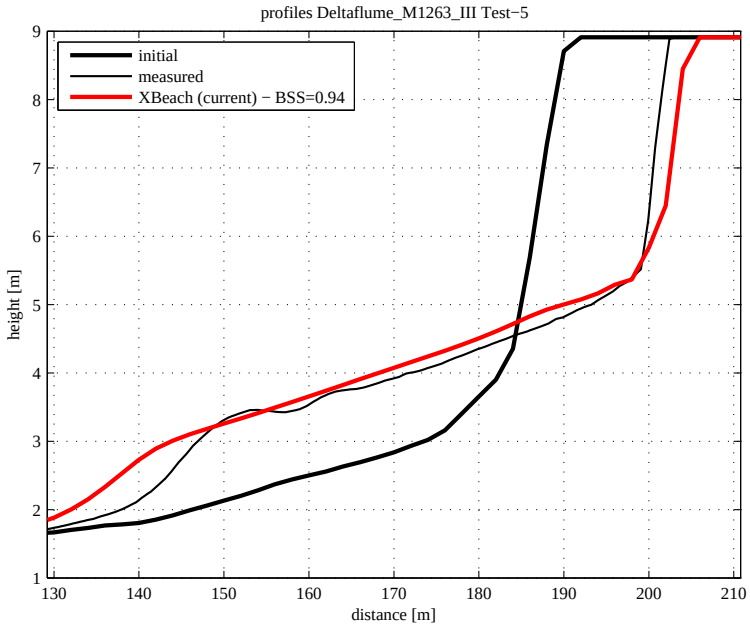

Figure 4.6: Final profile of test 5

4.1.3 LIP11D: Delta Flume 1994

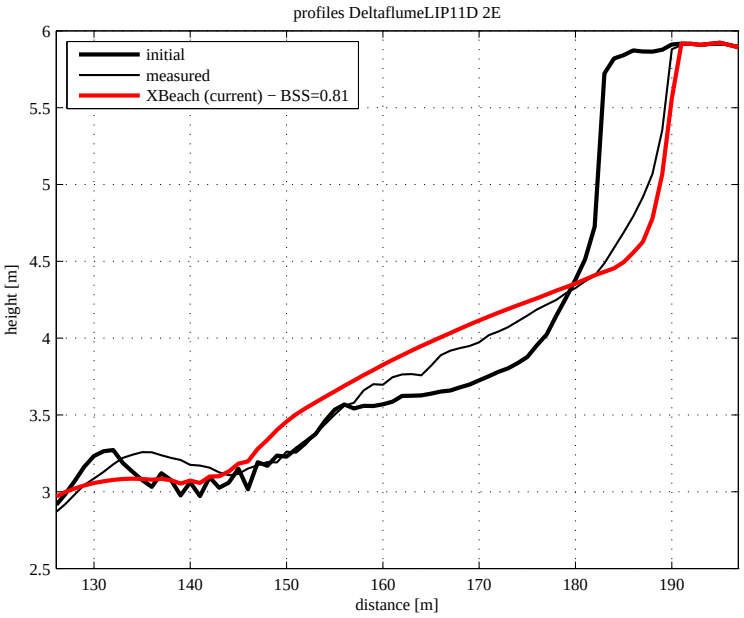

Figure 4.7: Final profile of test 2e

4.1.4 H4357: Delta Flume 2006

The 2006 Delta Flume experiments were performed to asses the effect of wave period on dune erosion(Van Gent et al., 2008). The tests were performed at a depth scale of 6 and with both Pierson-Moskowitz and double-peaked (DP01 and DP02) wave spectra. Results are shown in Figure 4.8 to Figure 4.13.

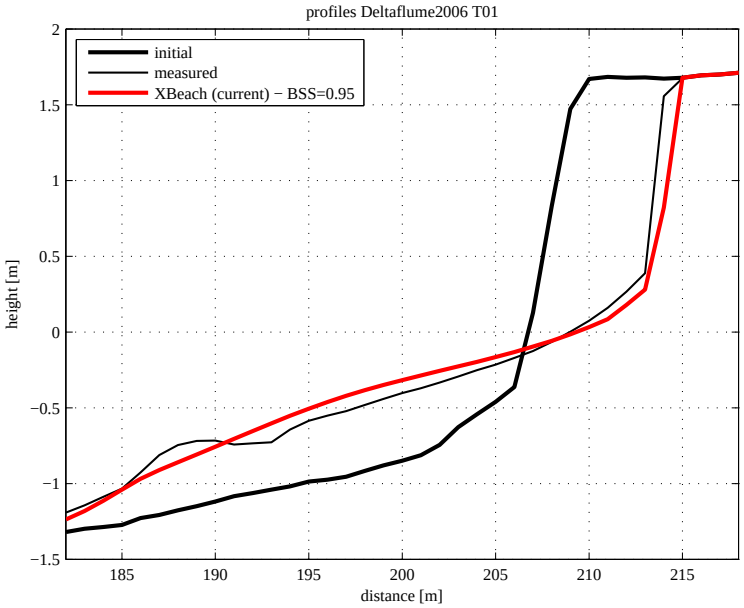

Figure 4.8: Final profile of test T01

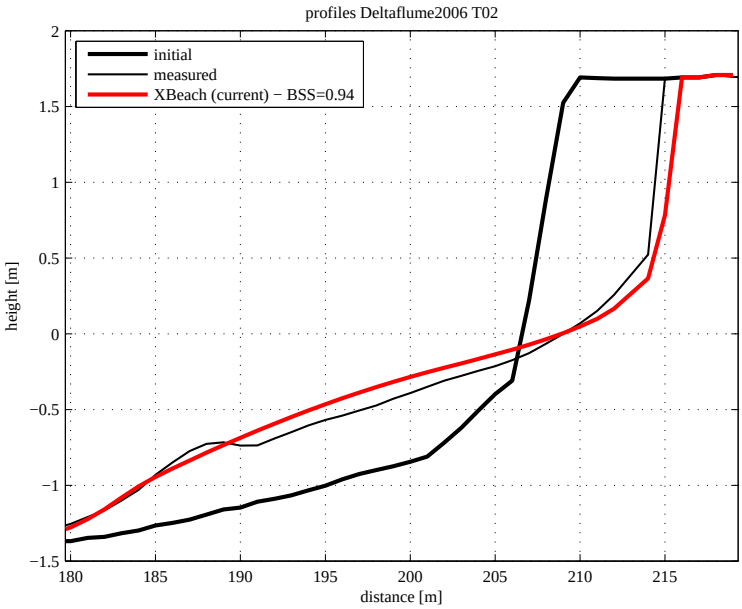

Figure 4.9: Final profile of test T02

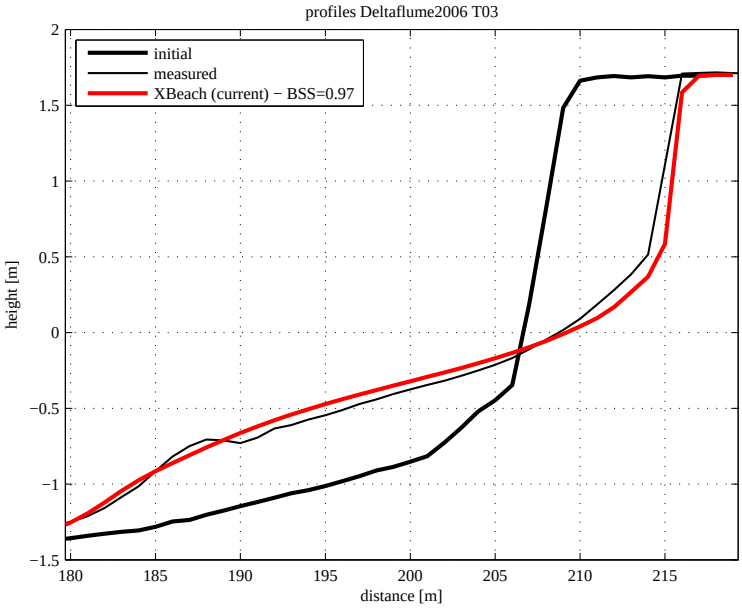

Figure 4.10: Final profile of test T03

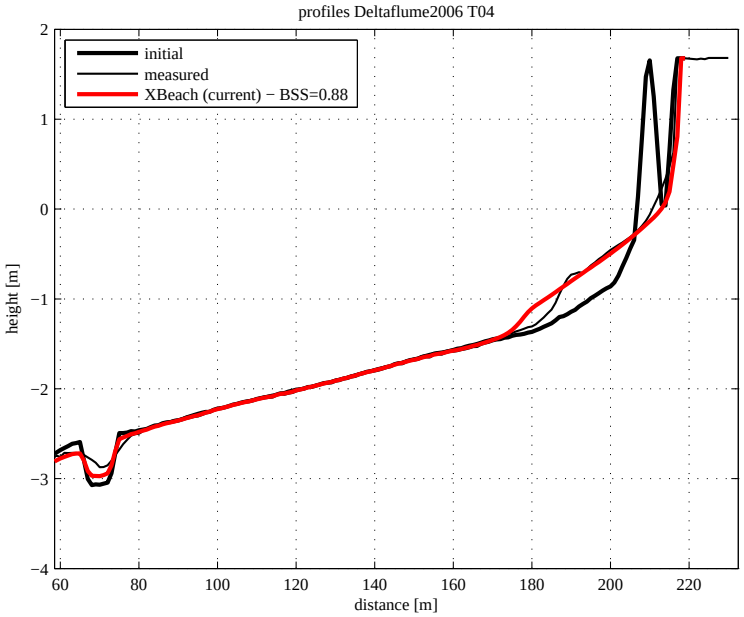

Figure 4.11: Final profile of test T04

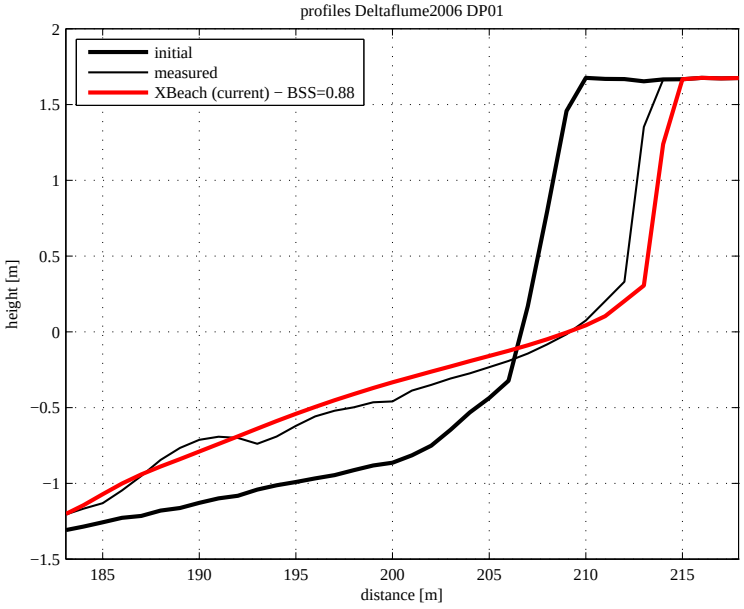

Figure 4.12: Final profile of test DP01

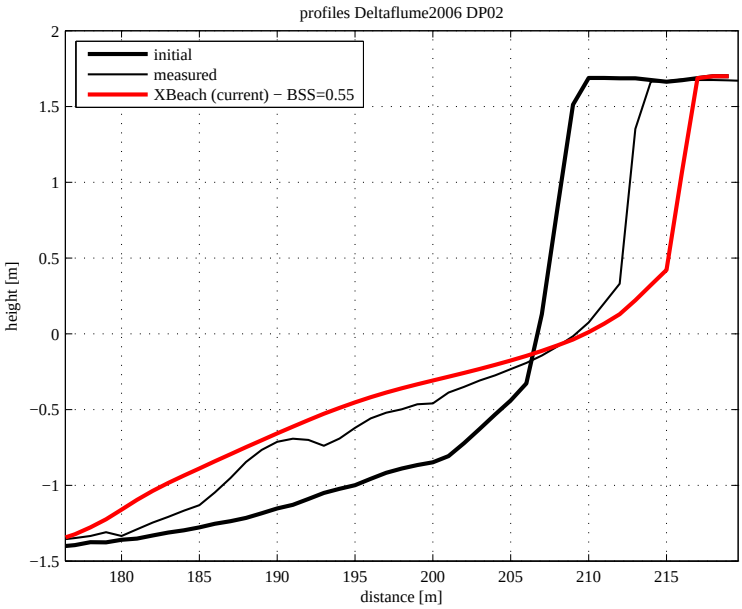

Figure 4.13: Final profile of test DP02

4.1.5 Grosse Wellen Kanal 1986

These figures and tables are generated by the automated XBeach skillbed.
Something has gone wrong, so sadly no figure or table could be generated.

Figure 4.14: Final profile of test T01

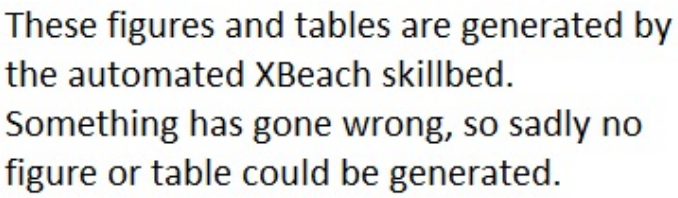

Figure 4.15: Final profile of test T02

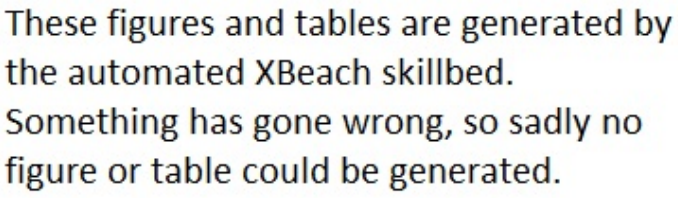

Figure 4.16: Final profile of test T03

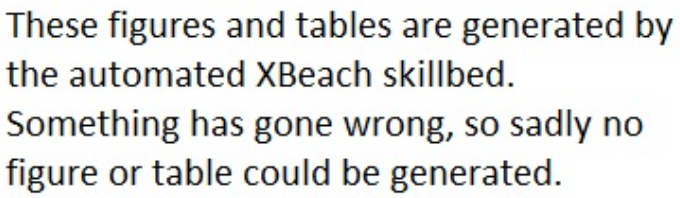

Figure 4.17: Final profile of test T04

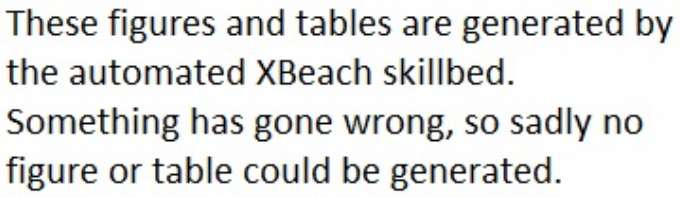

Figure 4.18: Final profile of test T05

These figures and tables are generated by the automated XBeach skillbed.
Something has gone wrong, so sadly no figure or table could be generated.

Figure 4.19: Final profile of test T06

4.1.6 Grosse Wellen Kanal 1998

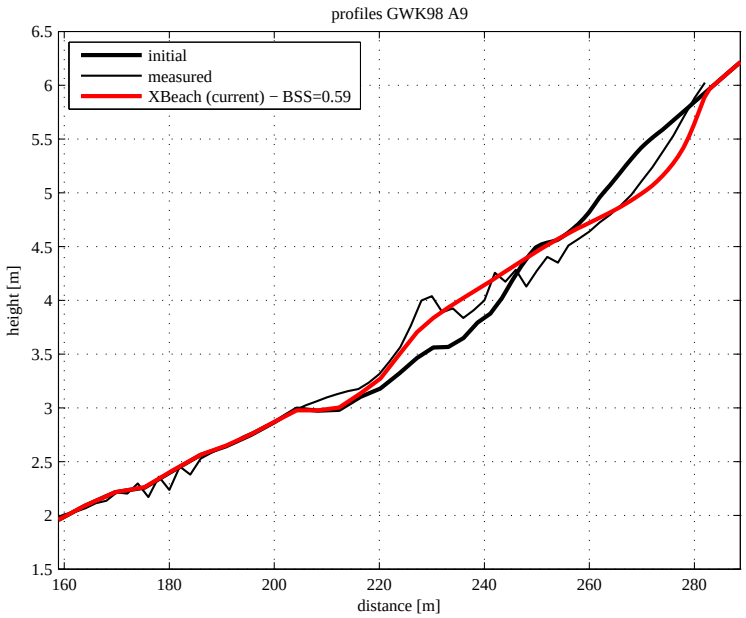

Figure 4.20: Final profile of test A9

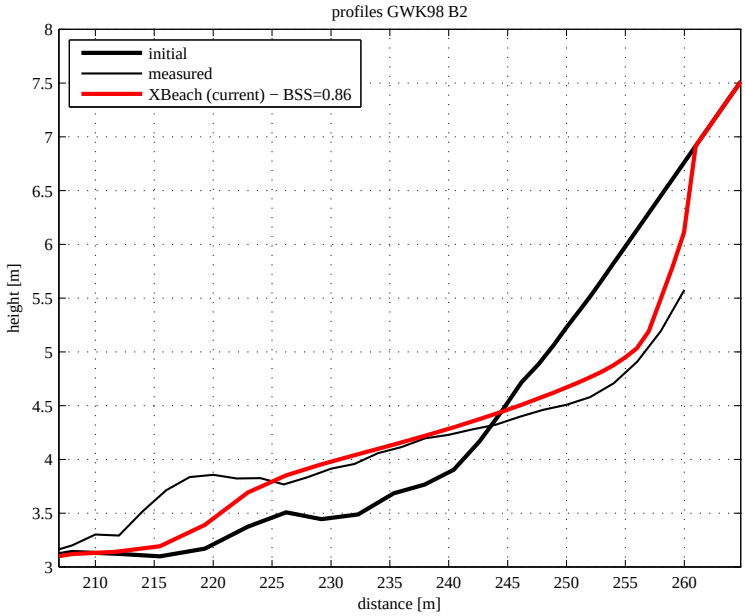

Figure 4.21: Final profile of test B2

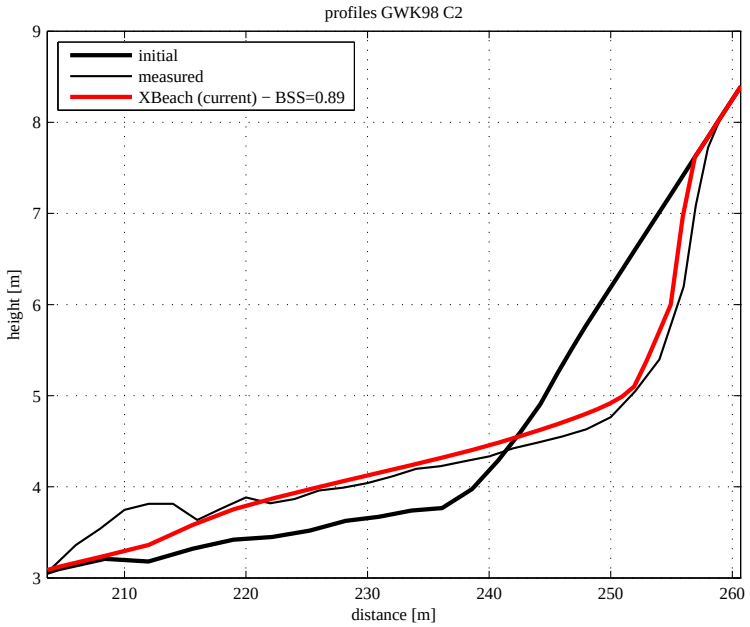

Figure 4.22: Final profile of test C2

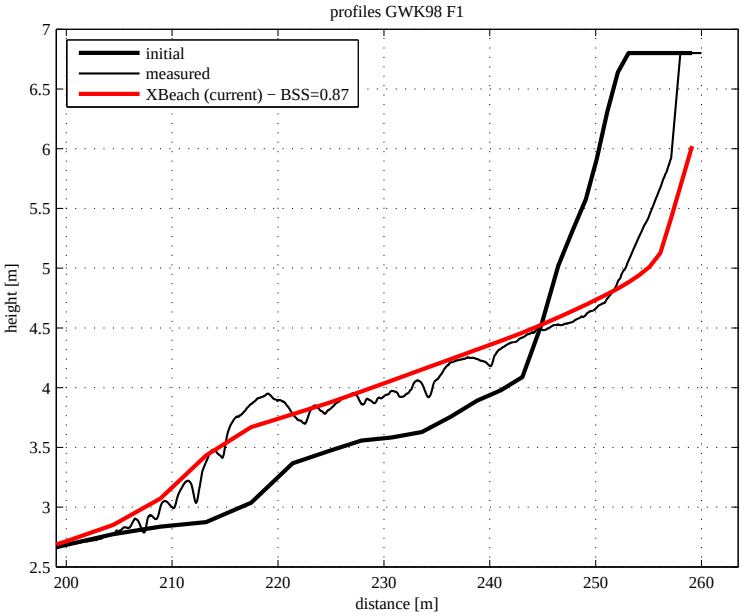

Figure 4.23: Final profile of test F1

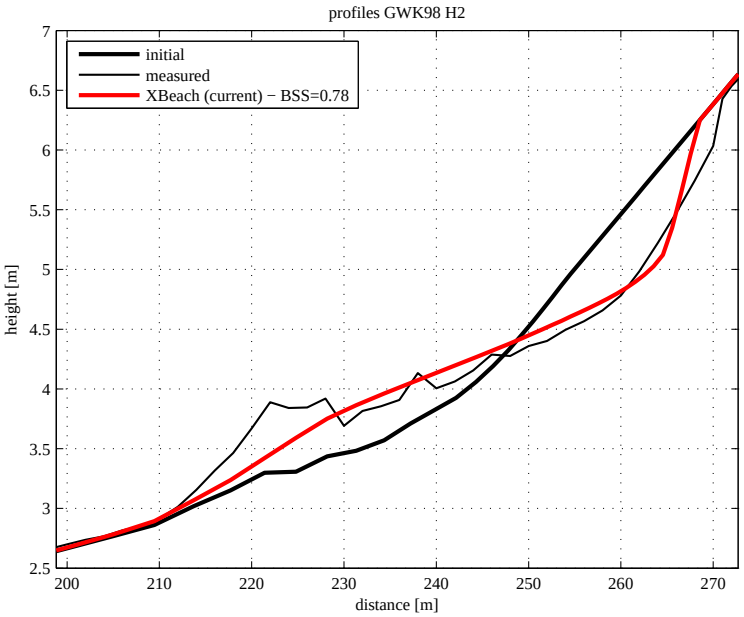

Figure 4.24: Final profile of test H2

4.2 Small scale laboratory tests

4.2.1 M1263 I: Wind Flume 1974-1975

The results depicted in Figure 4.25 to **??** were part of a series of experiments performed during 1974 and 1975 in the Wind Flume of Laboratory De Voorst in The Netherlands(Van de Graaff, 1976). During the experiments, depth scales of 84, 47 and 26 were used.

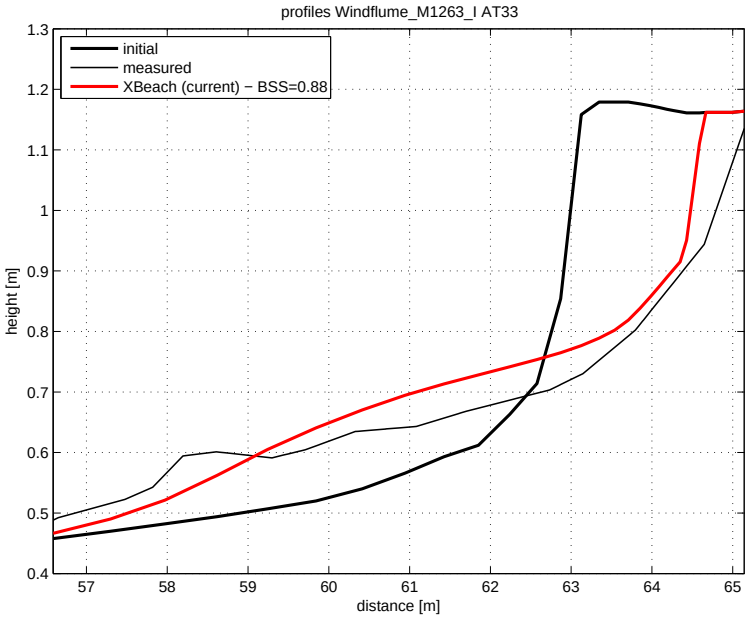

Figure 4.25: Final profile of test AT33

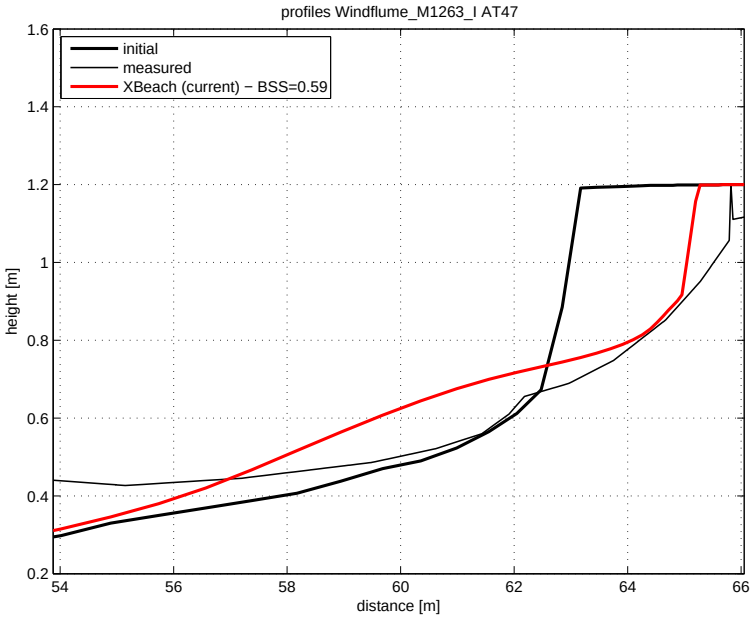

Figure 4.26: Final profile of test AT47

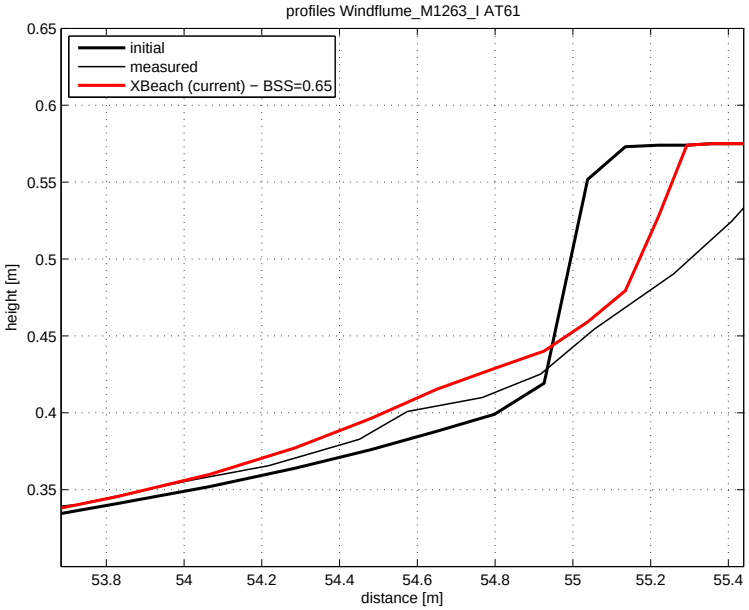

Figure 4.27: Final profile of test AT61

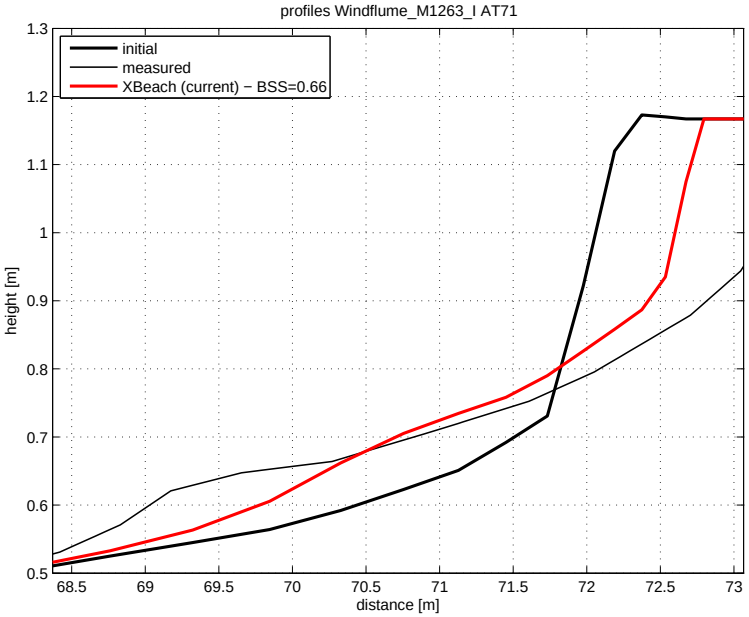

Figure 4.28: Final profile of test AT71

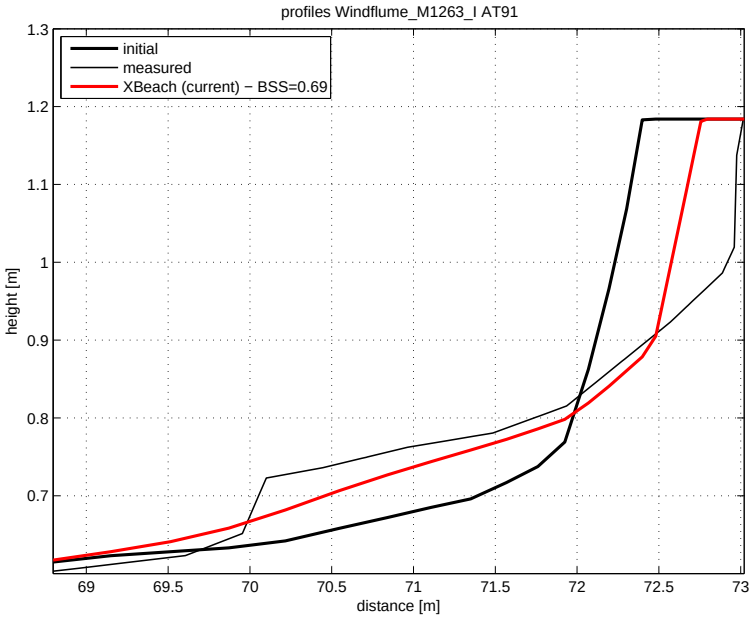

Figure 4.29: Final profile of test AT91

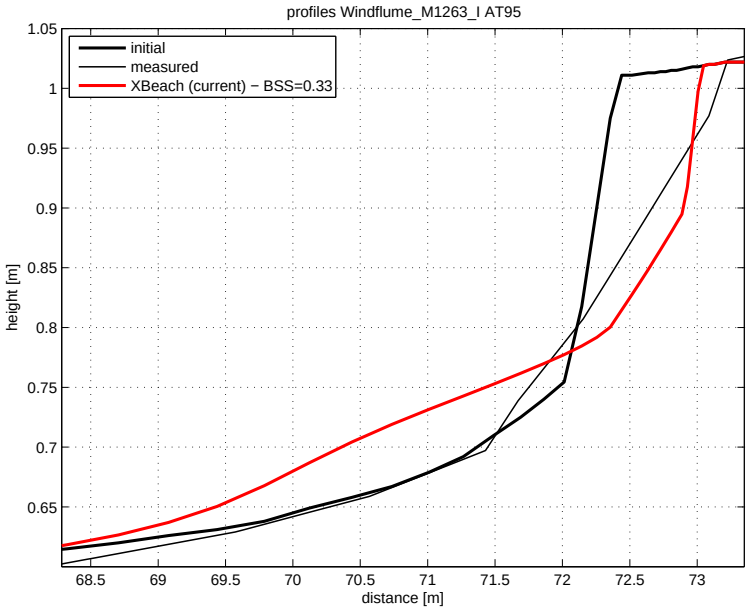

Figure 4.30: Final profile of test AT95

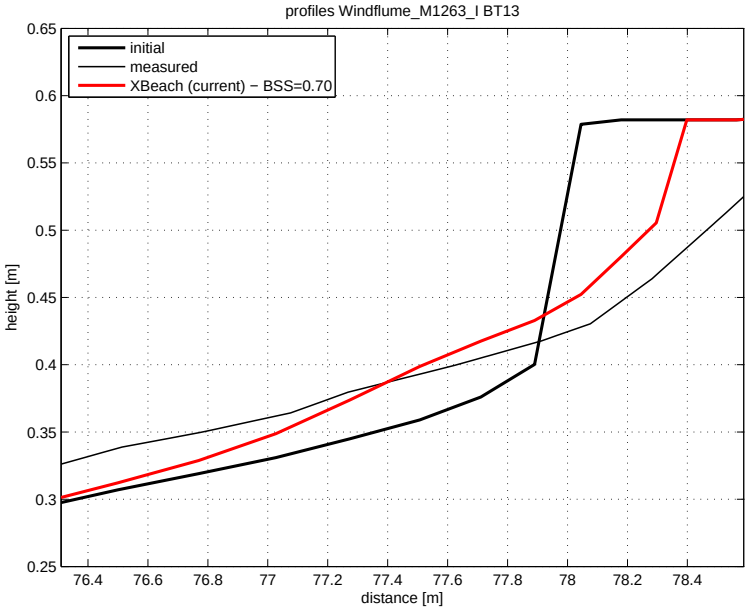

Figure 4.31: Final profile of test BT13

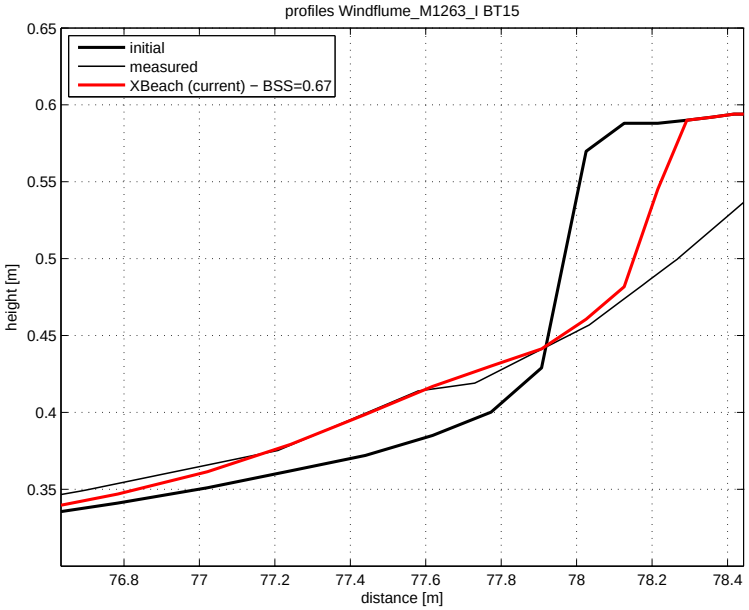

Figure 4.32: Final profile of test BT15

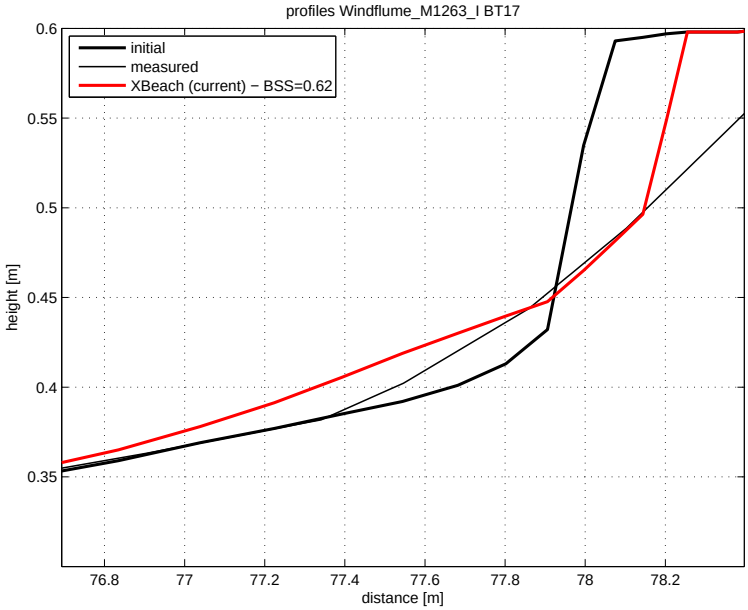

Figure 4.33: Final profile of test BT17

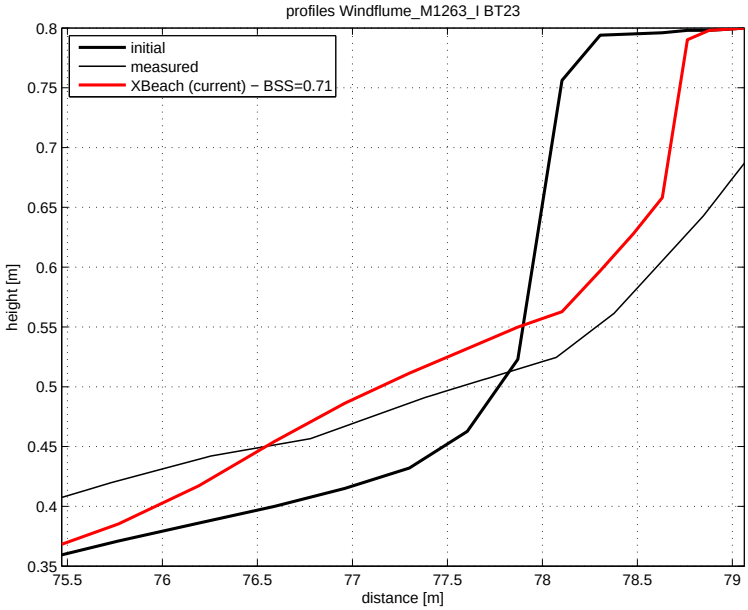

Figure 4.34: Final profile of test BT23

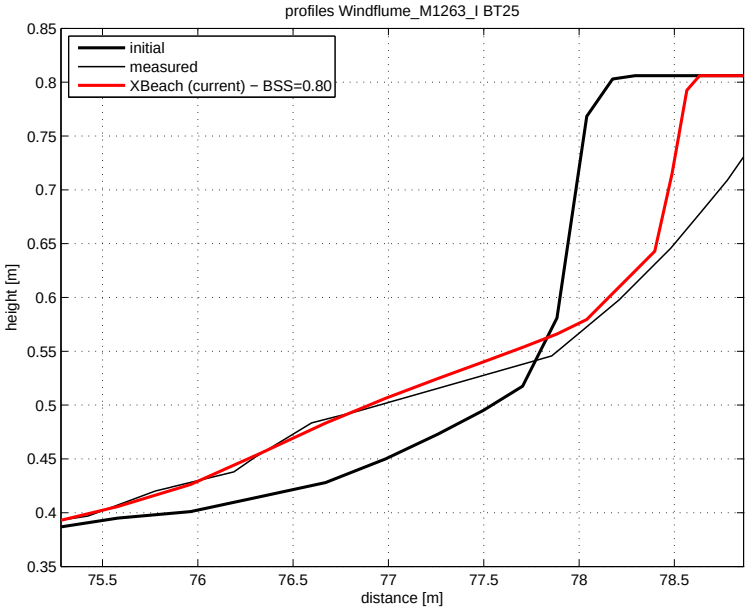

Figure 4.35: Final profile of test BT25

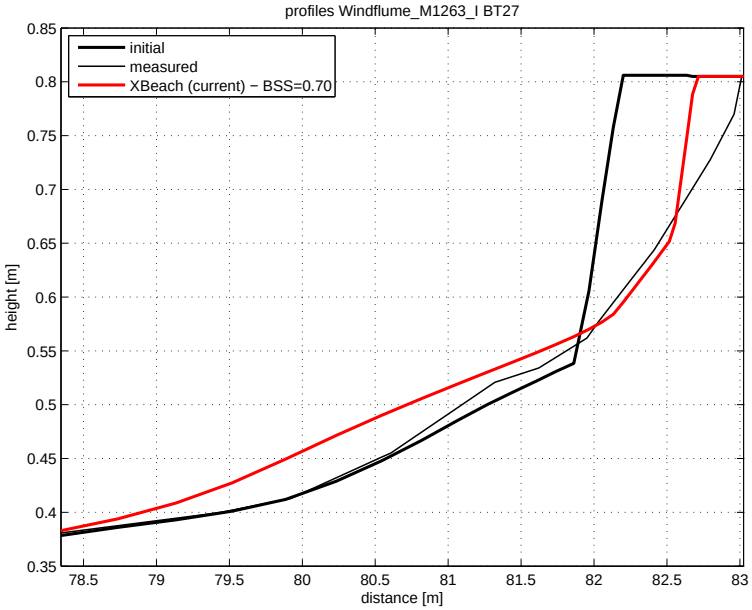

Figure 4.36: Final profile of test BT27

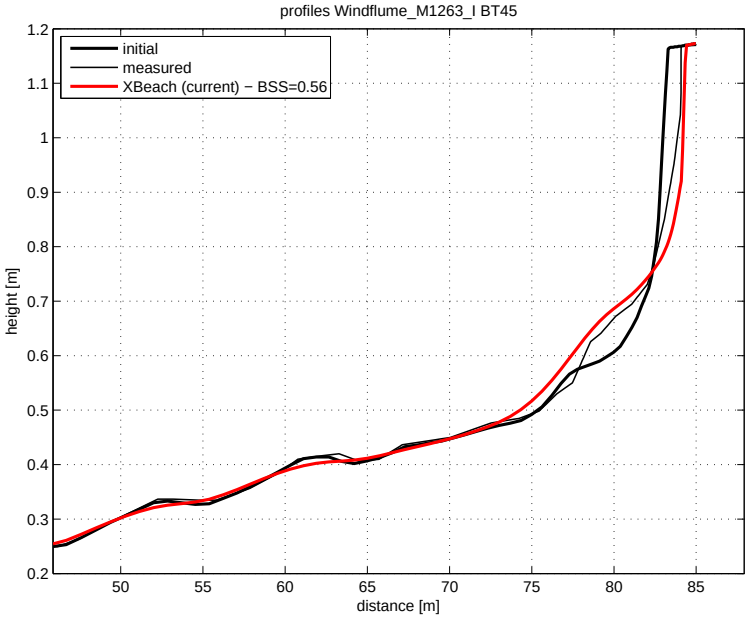

Figure 4.37: Final profile of test BT45

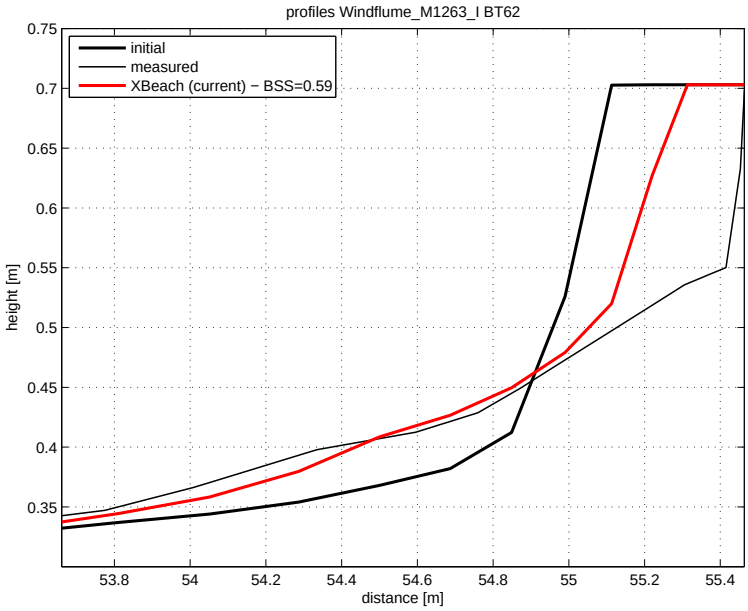

Figure 4.38: Final profile of test BT62

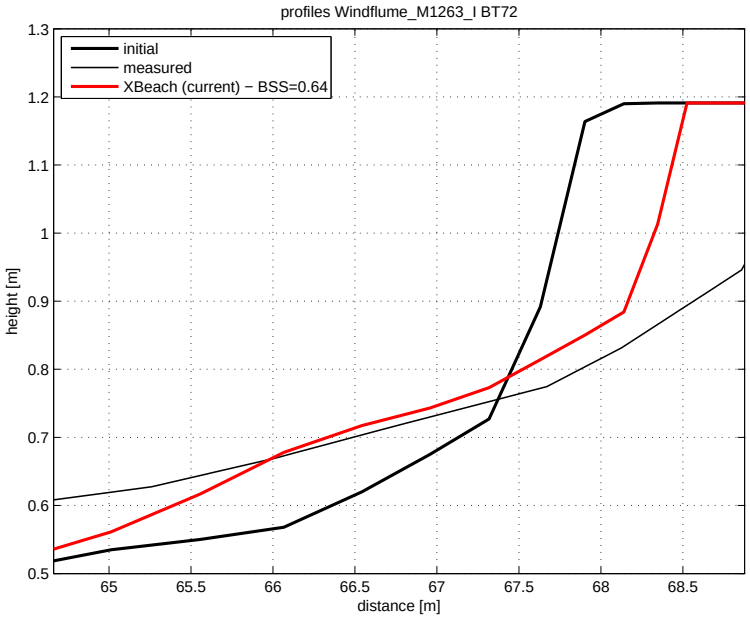

Figure 4.39: Final profile of test BT72

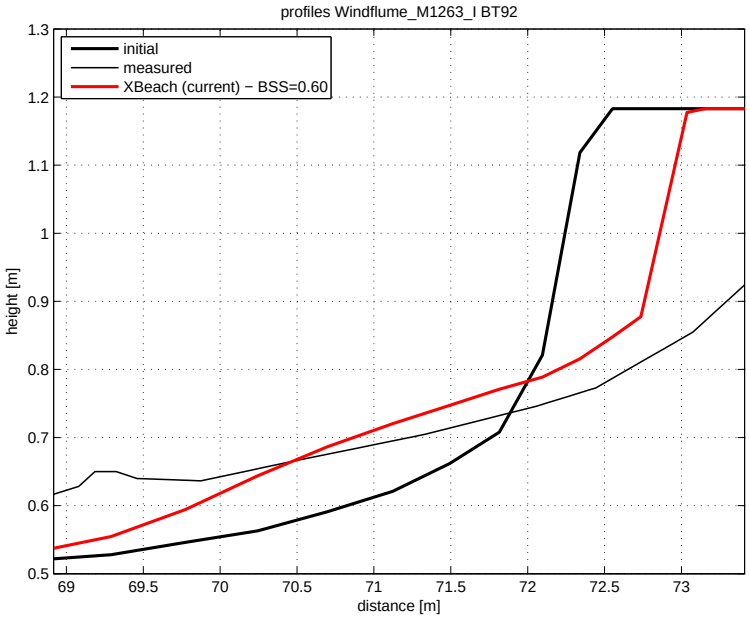

Figure 4.40: Final profile of test BT92

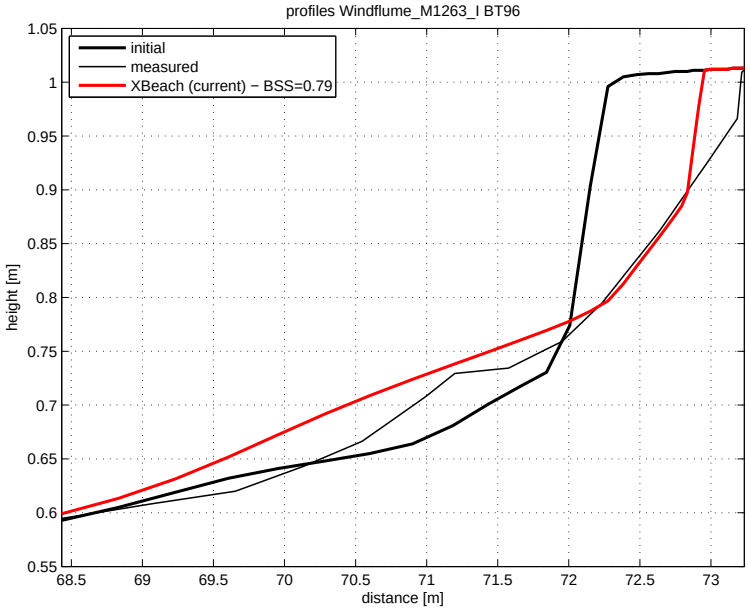

Figure 4.41: Final profile of test BT96

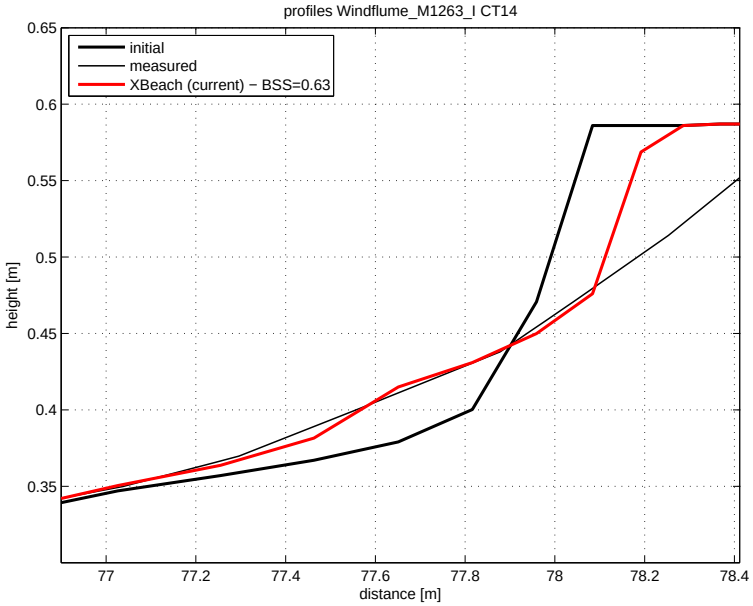

Figure 4.42: Final profile of test CT14

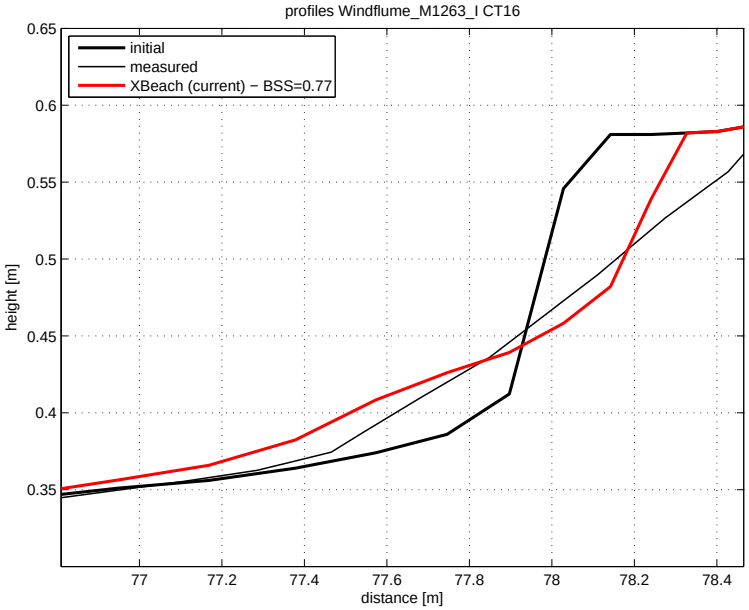

Figure 4.43: Final profile of test CT16

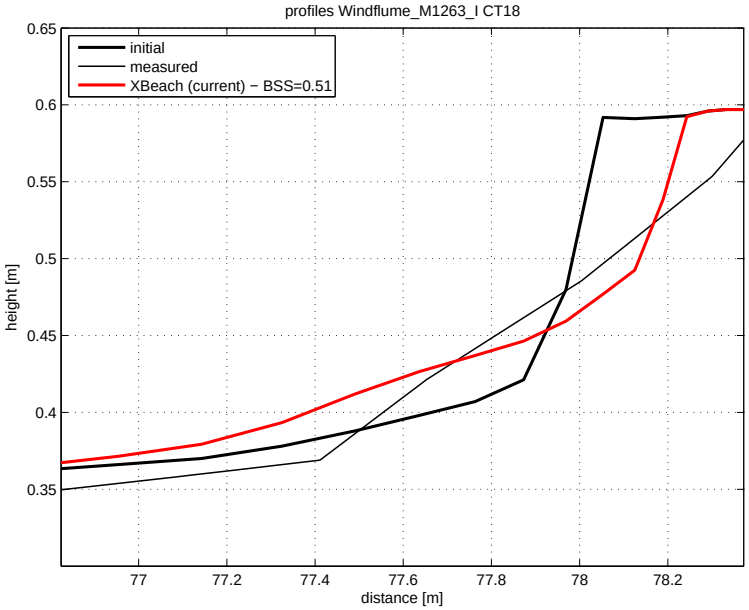

Figure 4.44: Final profile of test CT18

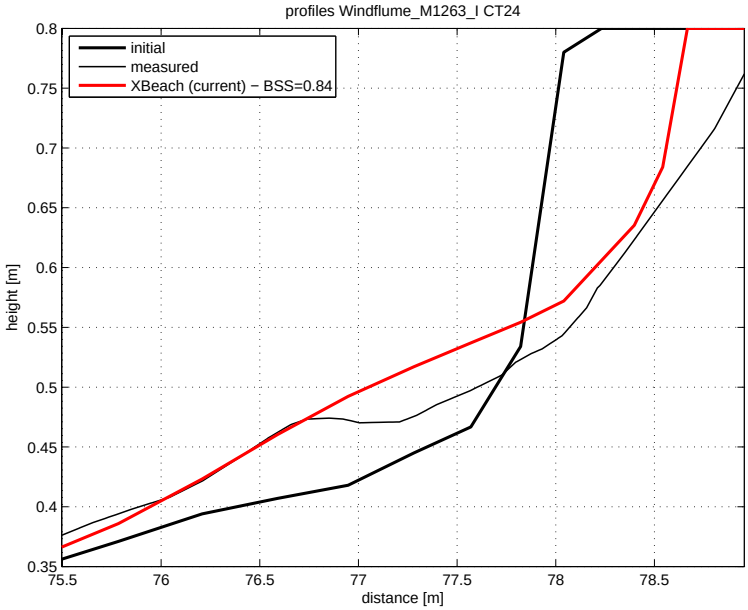

Figure 4.45: Final profile of test CT24

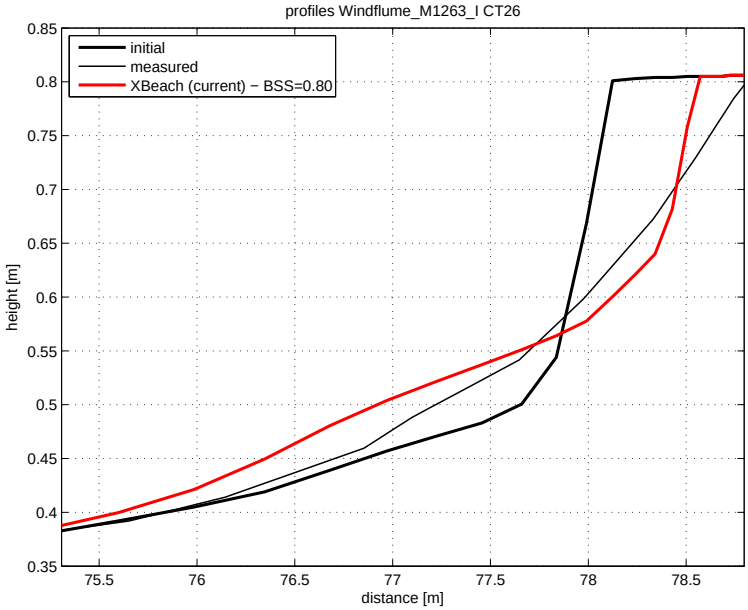

Figure 4.46: Final profile of test CT26

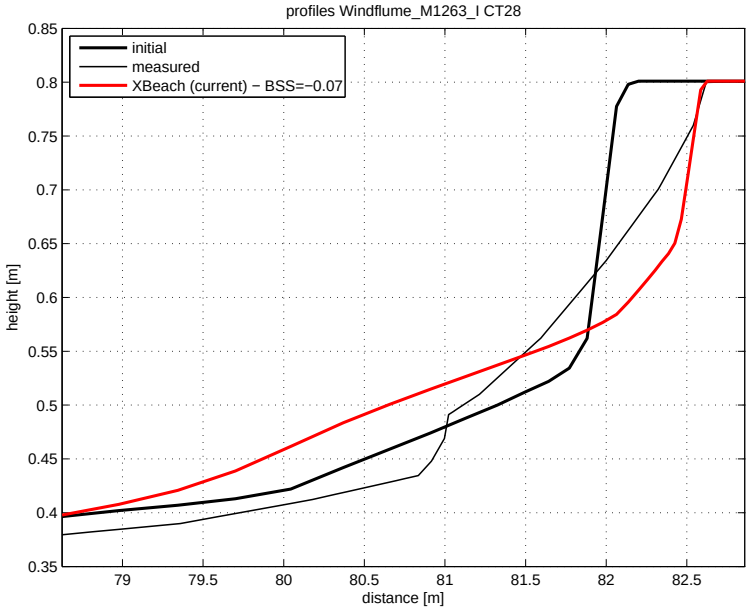

Figure 4.47: Final profile of test CT28

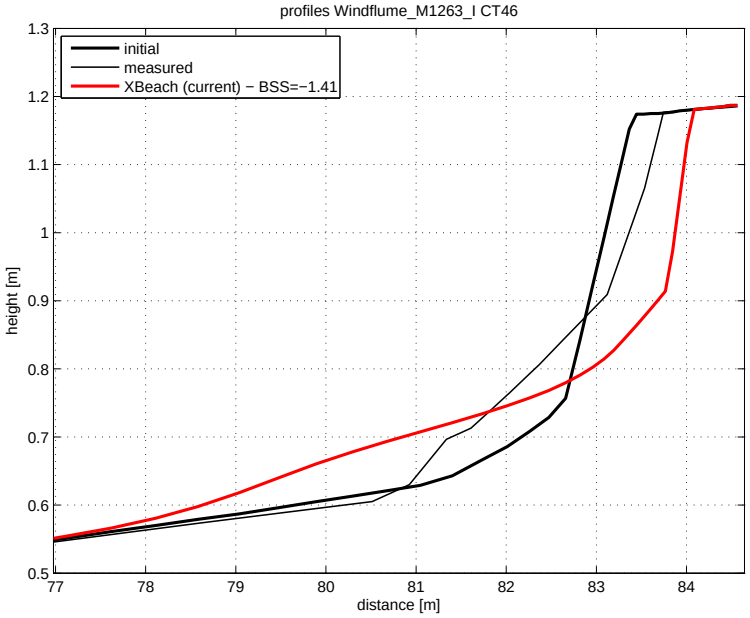

Figure 4.48: Final profile of test CT46

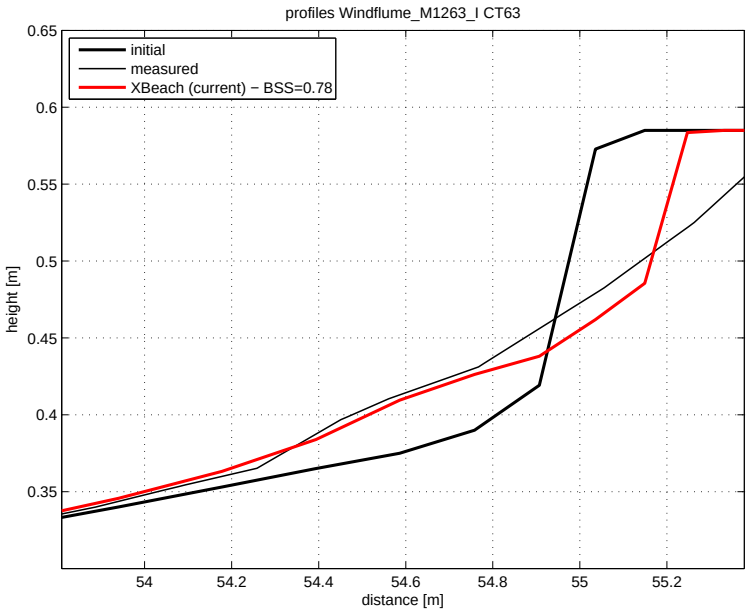

Figure 4.49: Final profile of test CT63

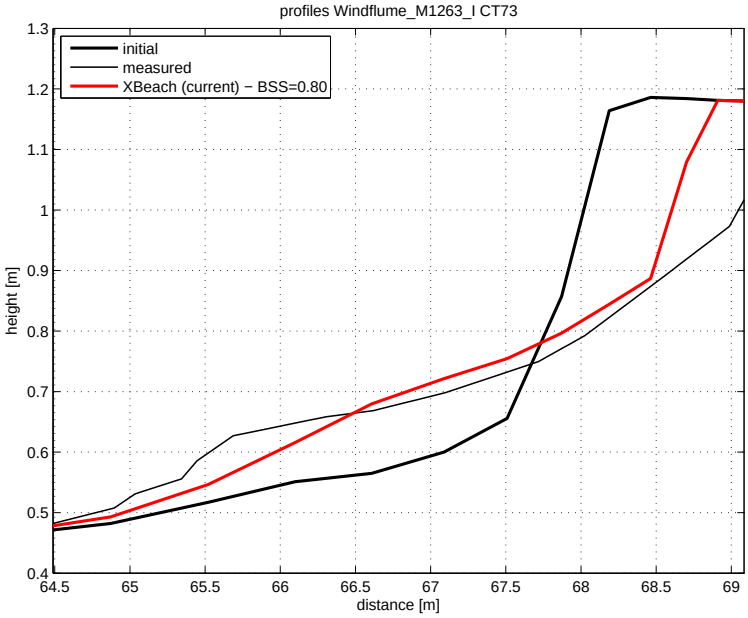

Figure 4.50: Final profile of test CT73

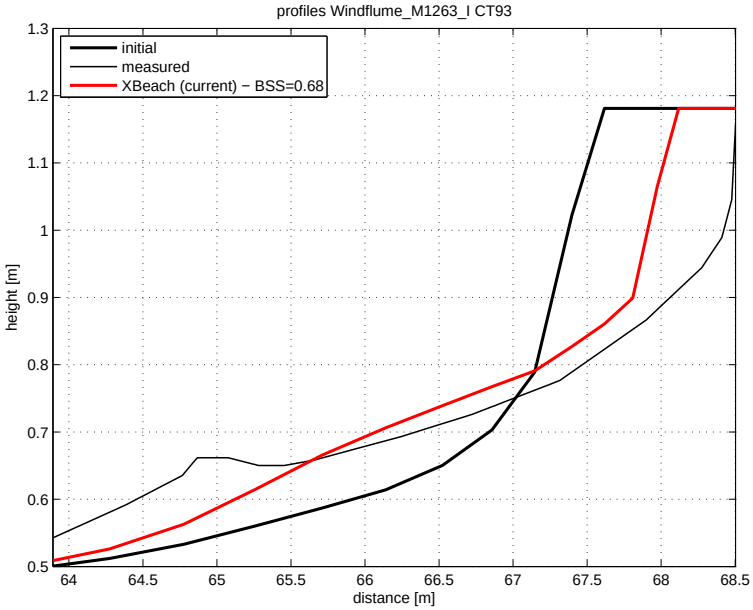

Figure 4.51: Final profile of test CT93

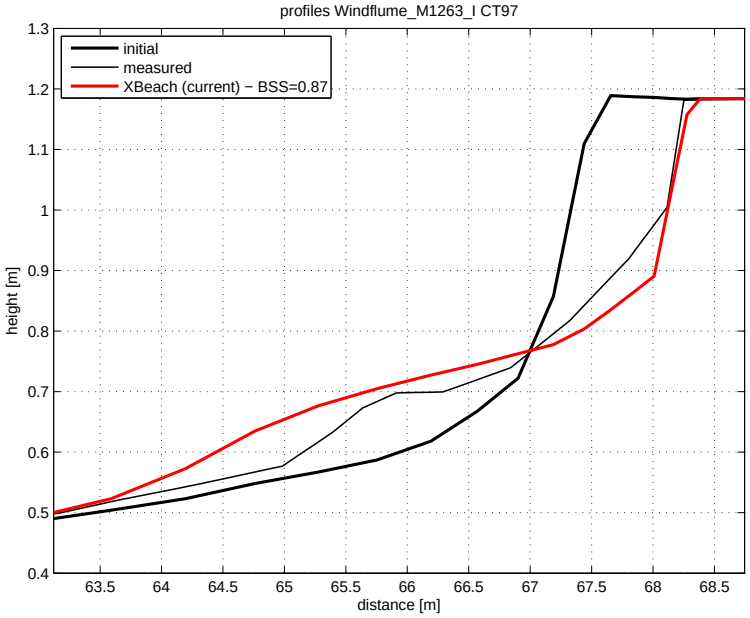

Figure 4.52: Final profile of test CT97

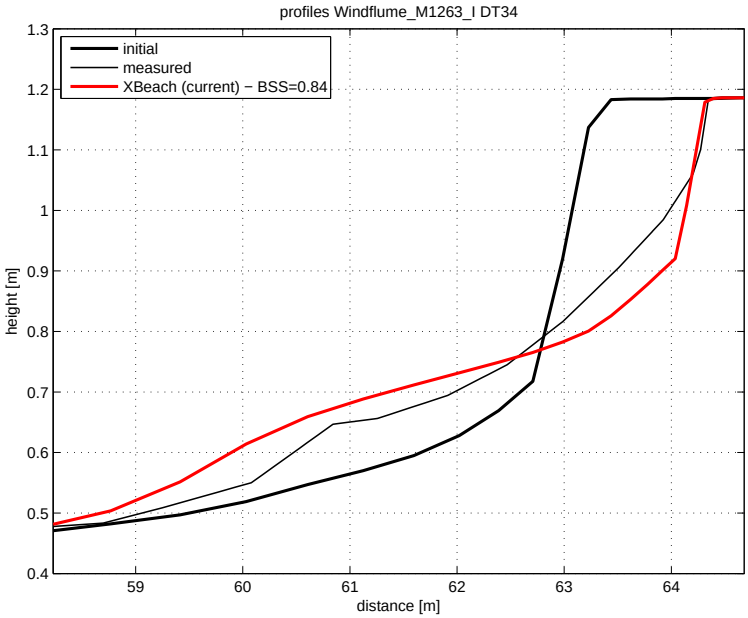

Figure 4.53: Final profile of test DT34

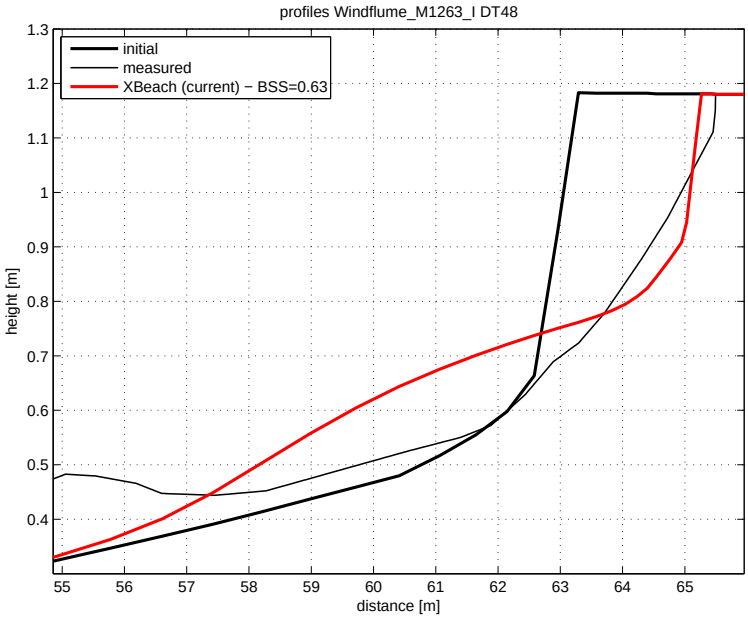

Figure 4.54: Final profile of test DT48

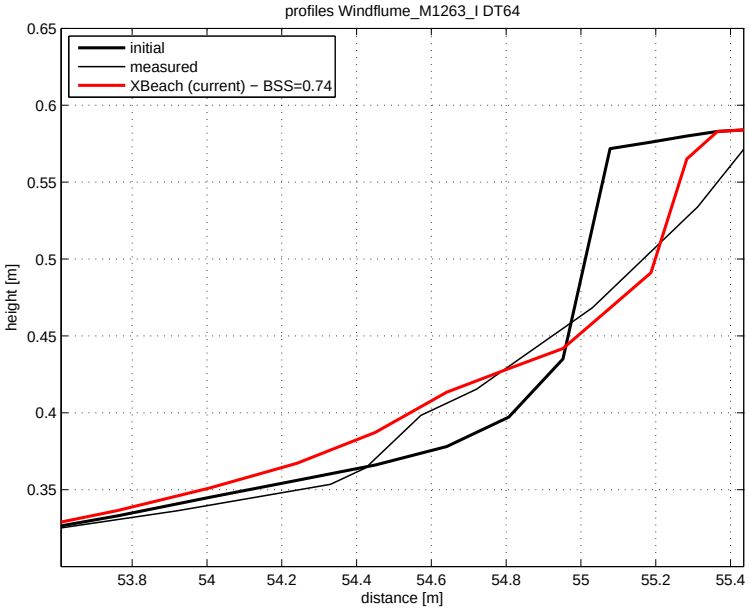

Figure 4.55: Final profile of test DT64

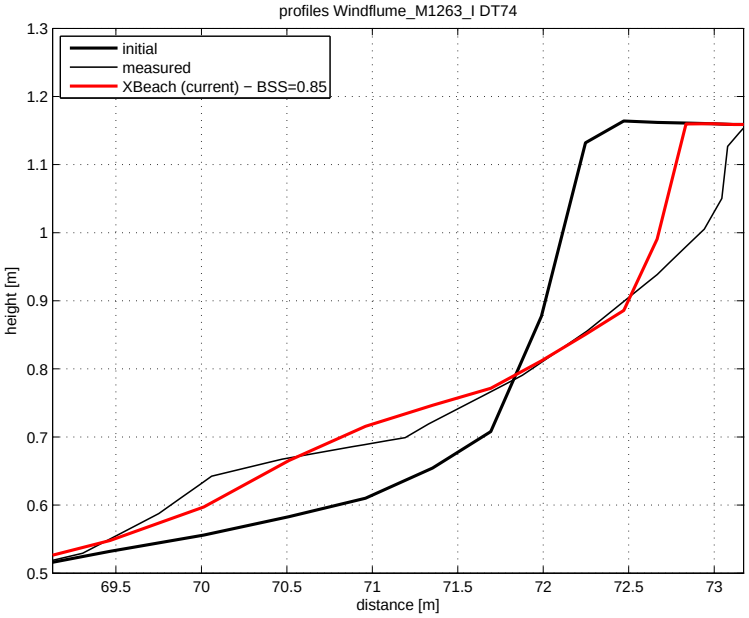

Figure 4.56: Final profile of test DT74

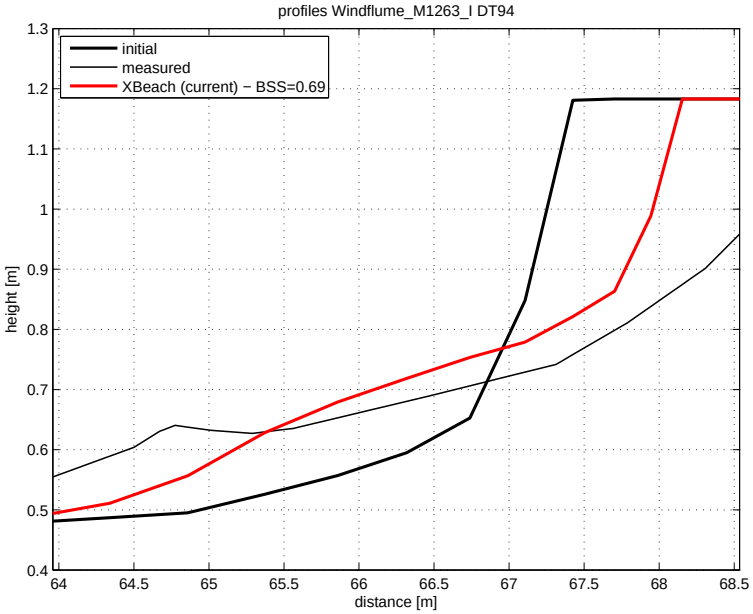

Figure 4.57: Final profile of test DT94

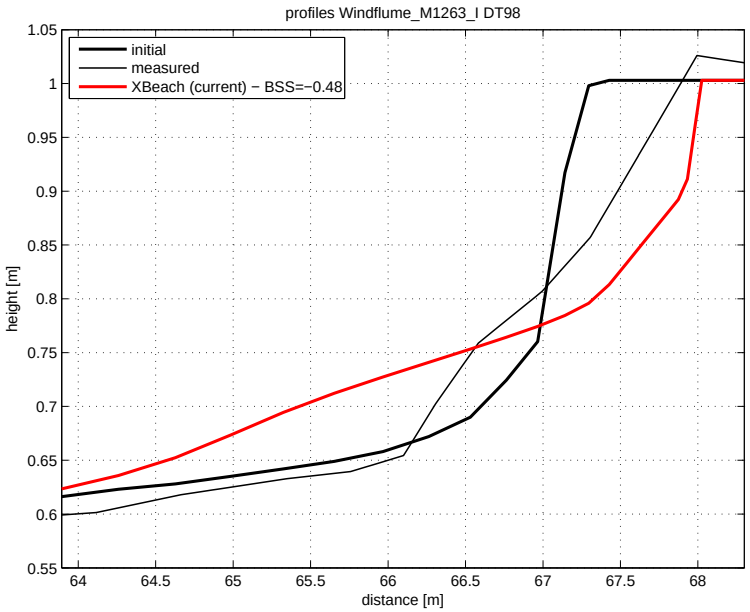

Figure 4.58: Final profile of test DT98

4.2.2 M1263 II: Wind Flume 1976-1977

Figure 4.59 to Figure 4.70 depict the tests performed in part II of the M1263 experiments, also in the Wind Flume and with depth scales of 84, 47 and 26(Vellinga, 1981b).

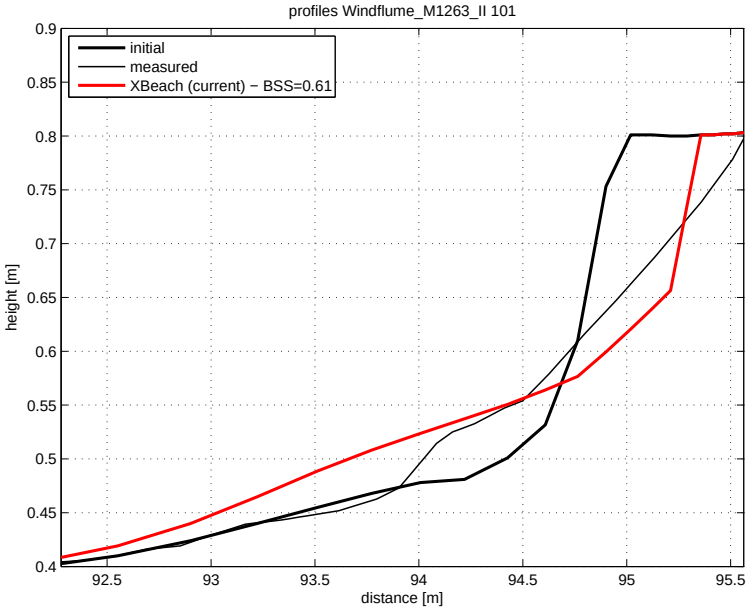

Figure 4.59: Final profile of test 101

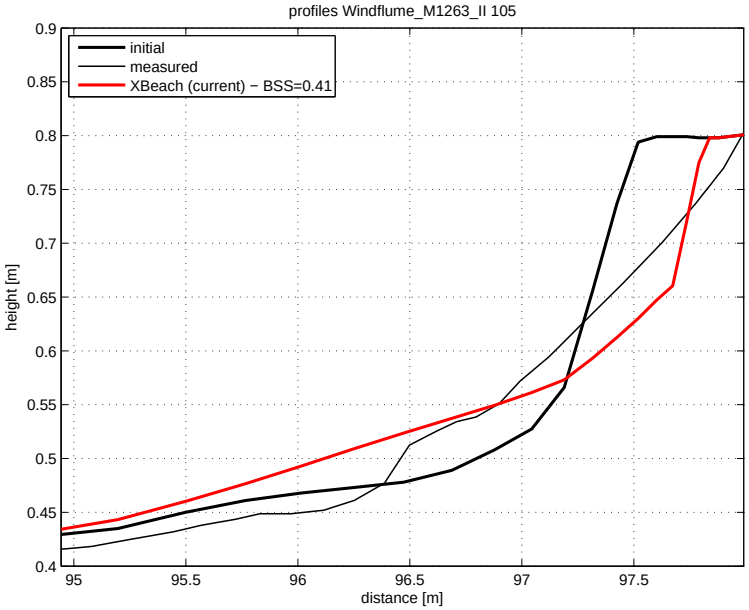

Figure 4.60: Final profile of test 105

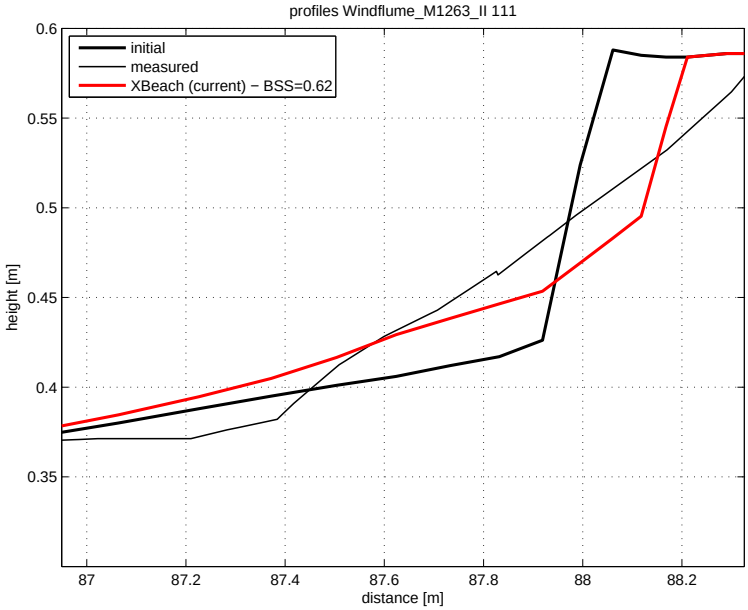

Figure 4.61: Final profile of test 111

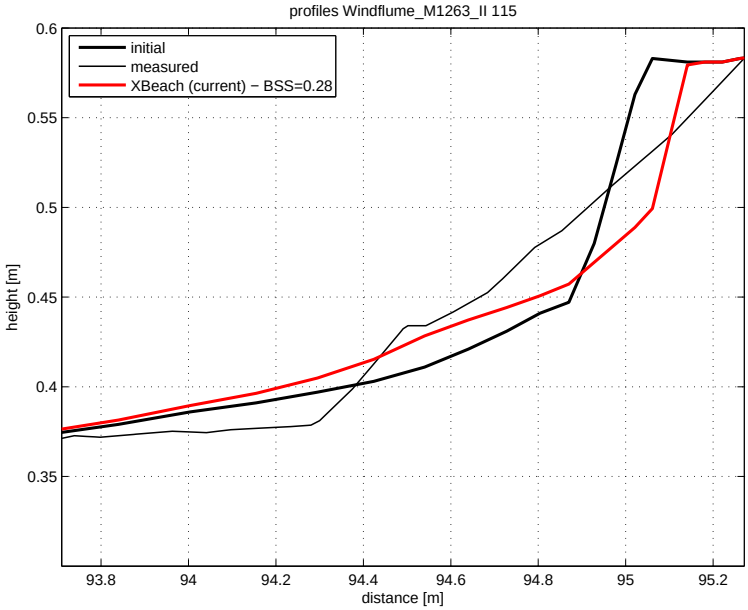

Figure 4.62: Final profile of test 115

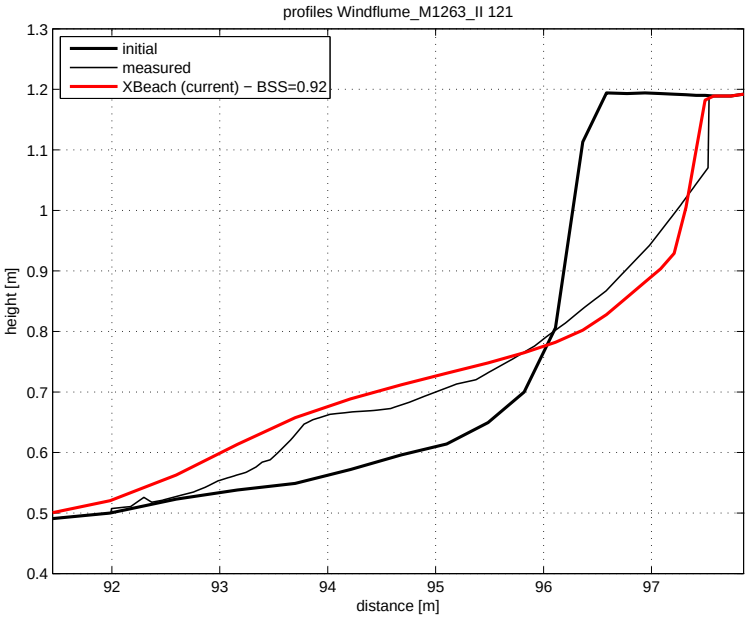

Figure 4.63: Final profile of test 121

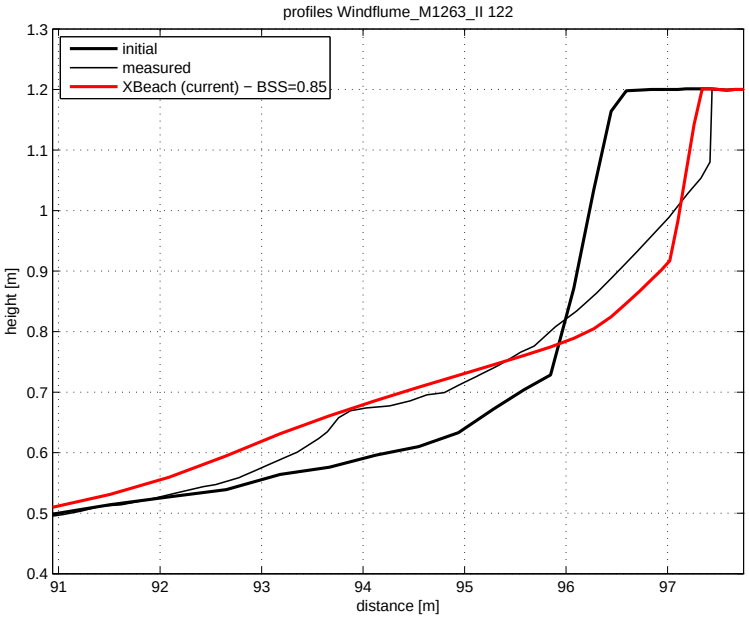

Figure 4.64: Final profile of test 122

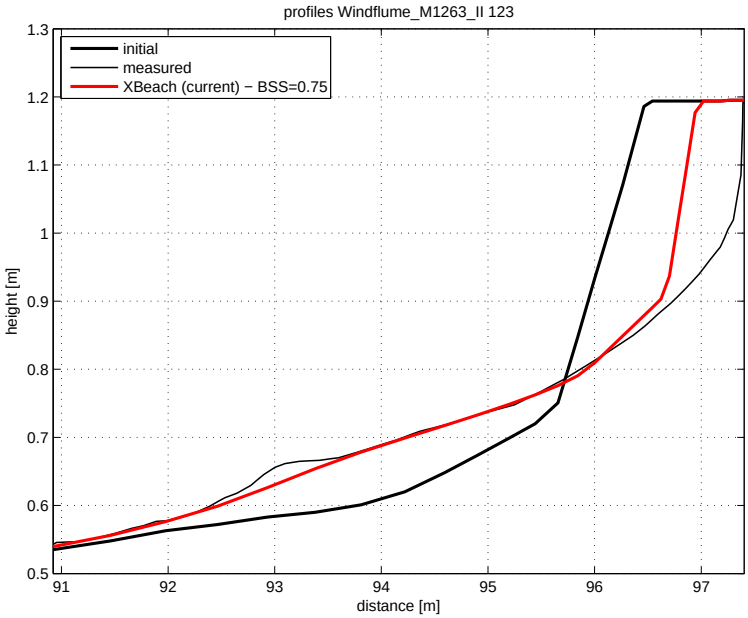

Figure 4.65: Final profile of test 123

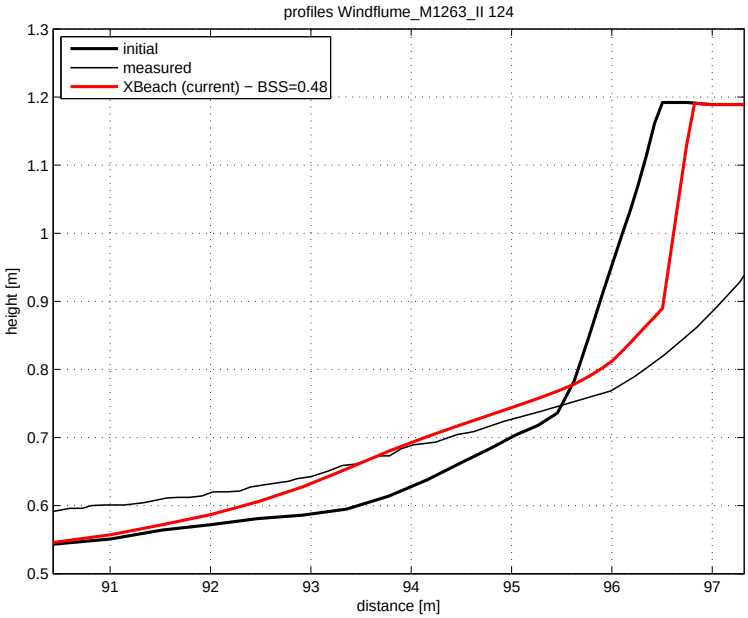

Figure 4.66: Final profile of test 124

These figures and tables are generated by the automated XBeach skillbed.
Something has gone wrong, so sadly no figure or table could be generated.

Figure 4.67: Final profile of test 125

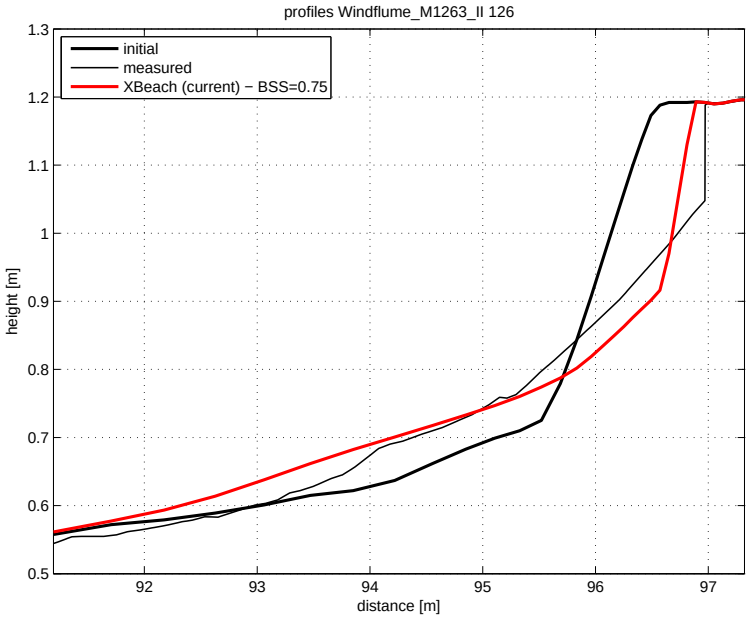

Figure 4.68: Final profile of test 126

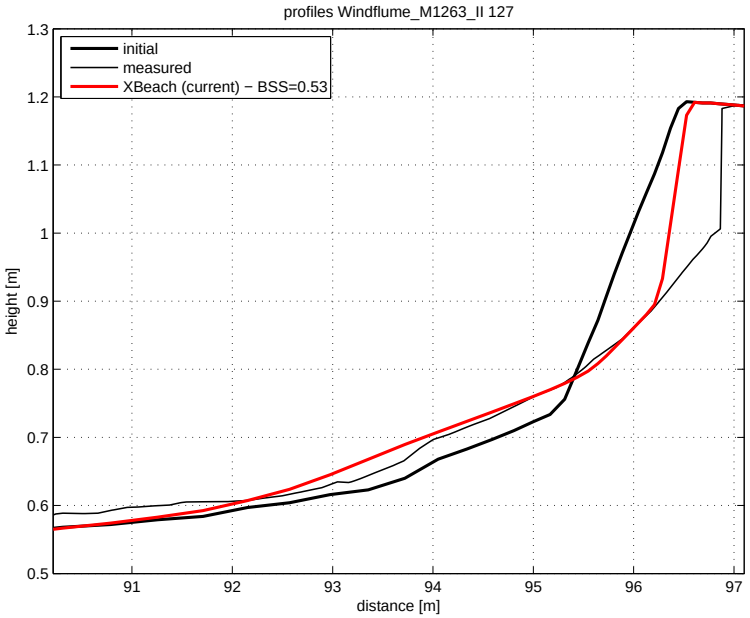

Figure 4.69: Final profile of test 127

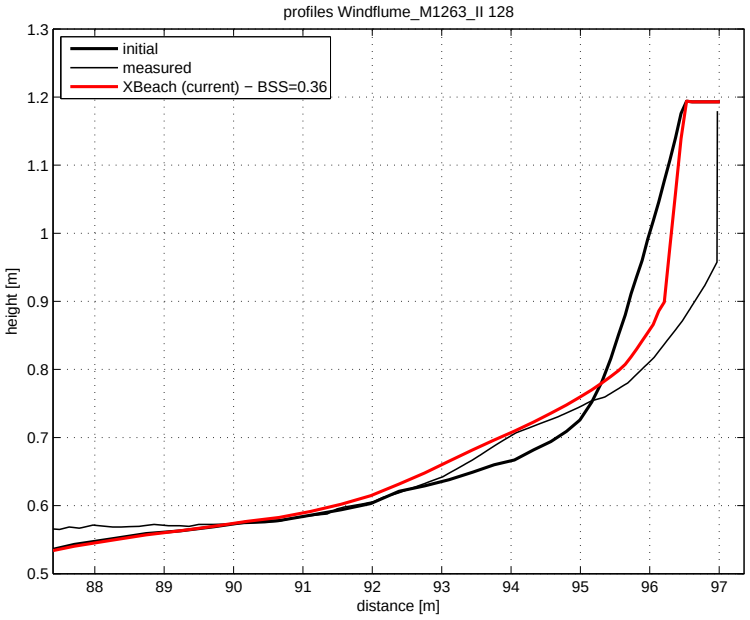

Figure 4.70: Final profile of test 128

4.2.3 M1819 I: Scheldt Flume 1981

In 1981, small scale dune erosion experiments (with a depth scale of 30) were performed in the Scheldt Flume of Laboratory De Voorst in The Netherlands(Tilmans, 1982), the results of which are shown in Figure 4.71 to Figure 4.93.

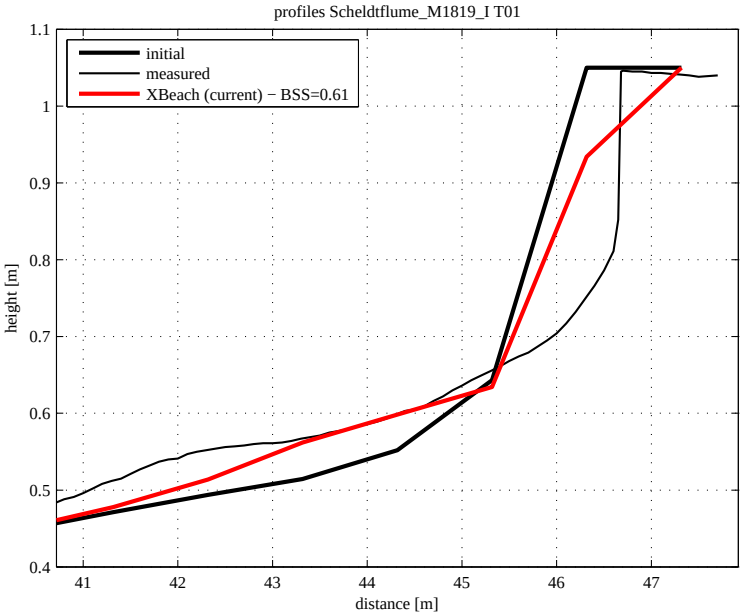

Figure 4.71: Final profile of test T01

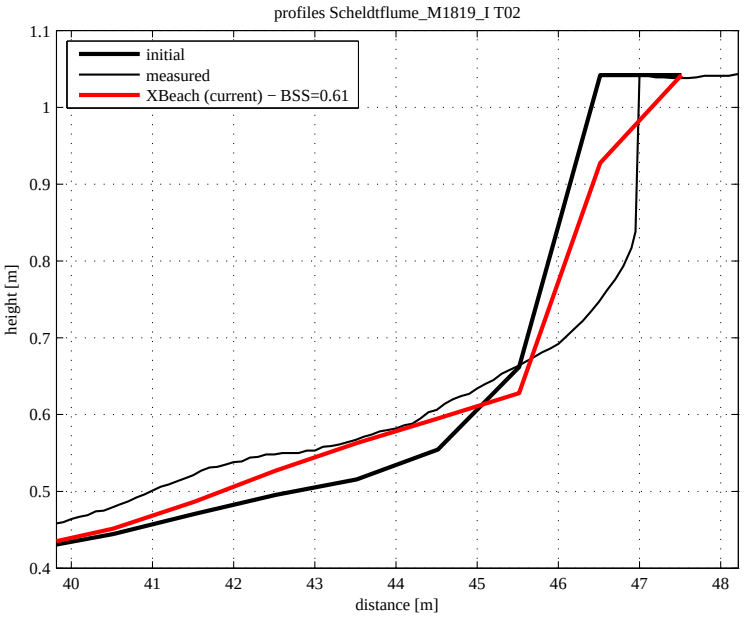

Figure 4.72: Final profile of test T02

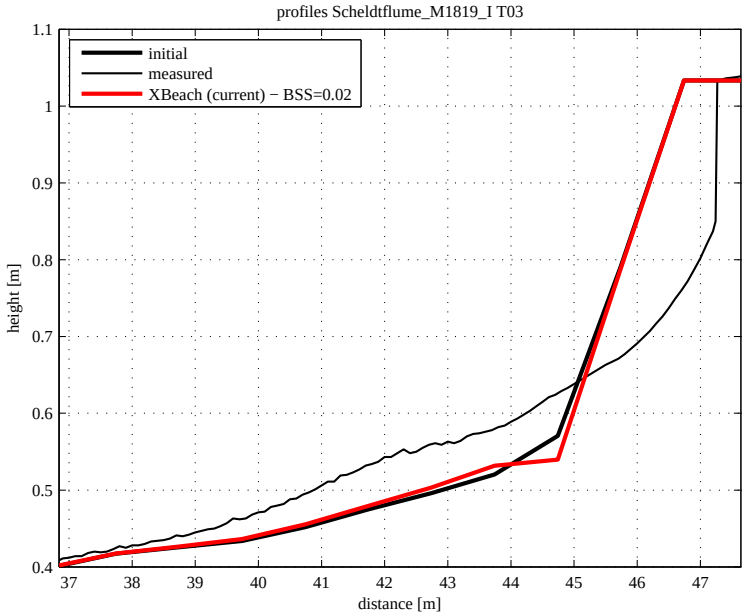

Figure 4.73: Final profile of test T03

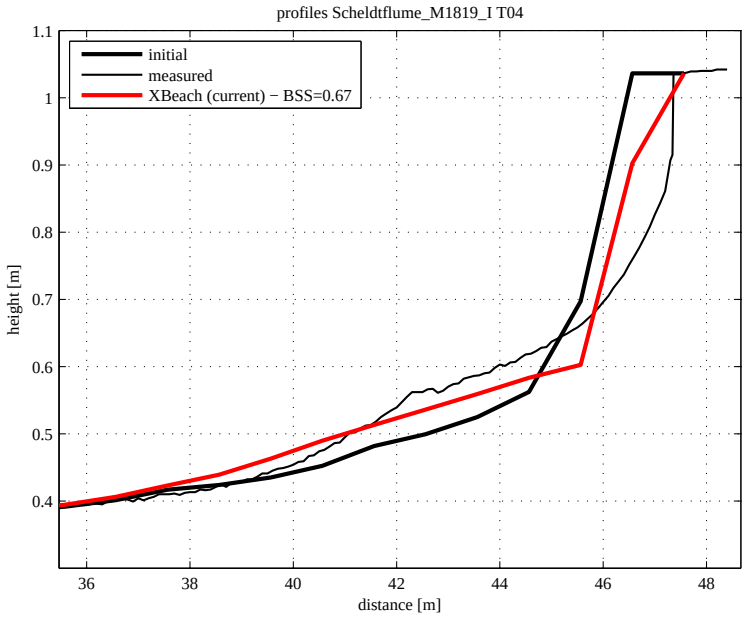

Figure 4.74: Final profile of test T04

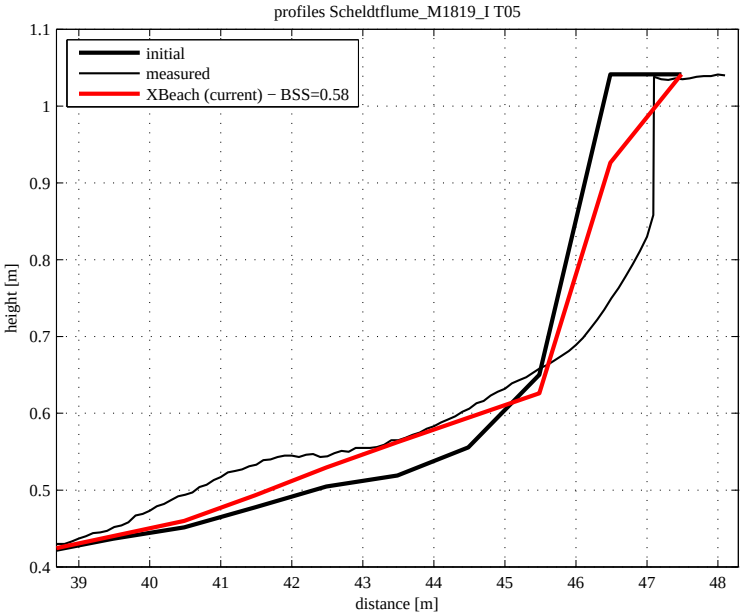

Figure 4.75: Final profile of test T05

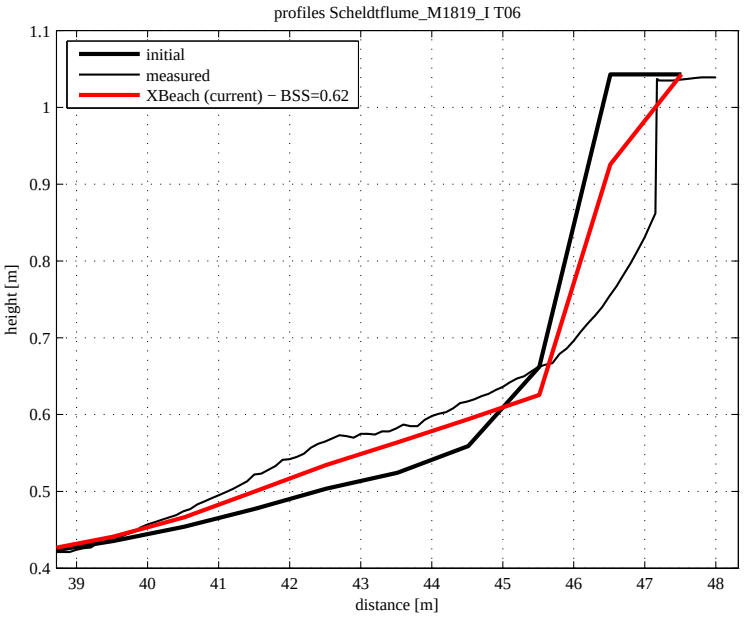

Figure 4.76: Final profile of test T06

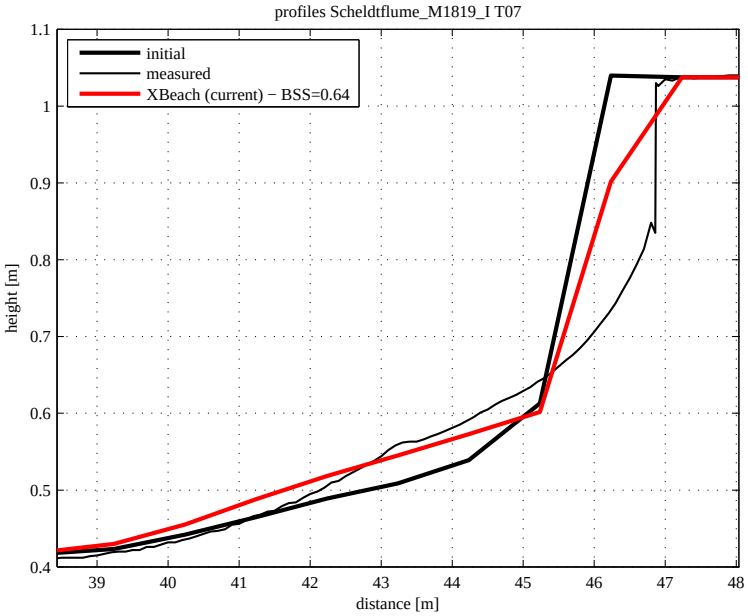

Figure 4.77: Final profile of test T07

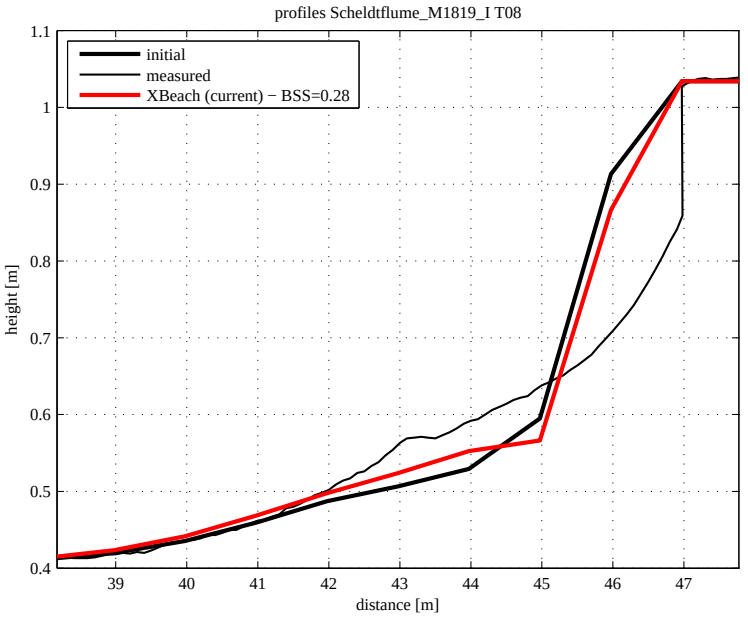

Figure 4.78: Final profile of test T08

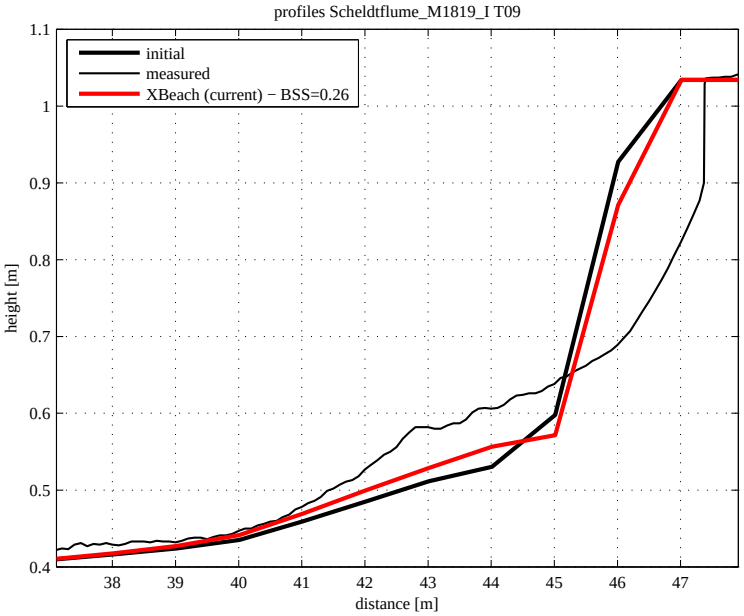

Figure 4.79: Final profile of test T09

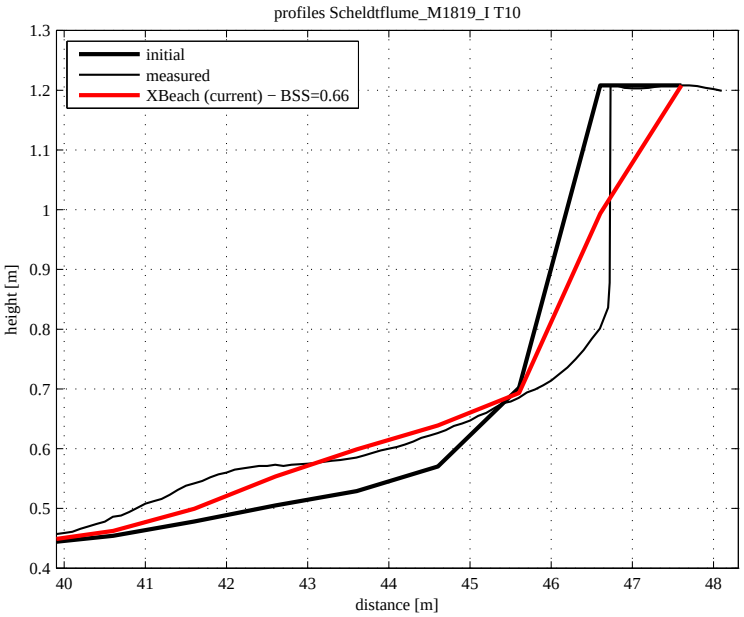

Figure 4.80: Final profile of test T10

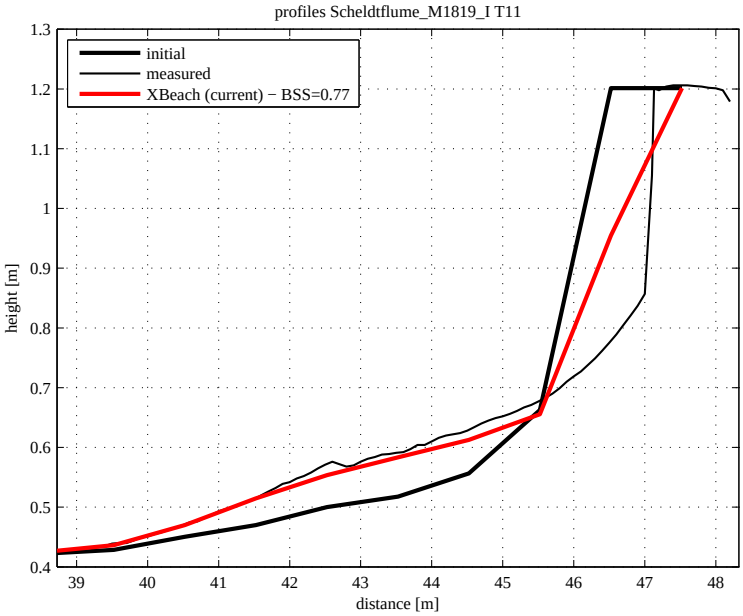

Figure 4.81: Final profile of test T11

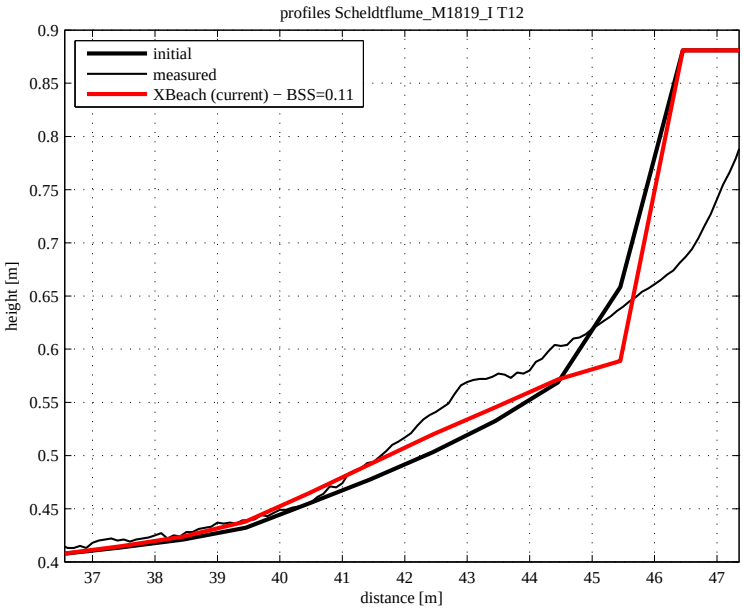

Figure 4.82: Final profile of test T12

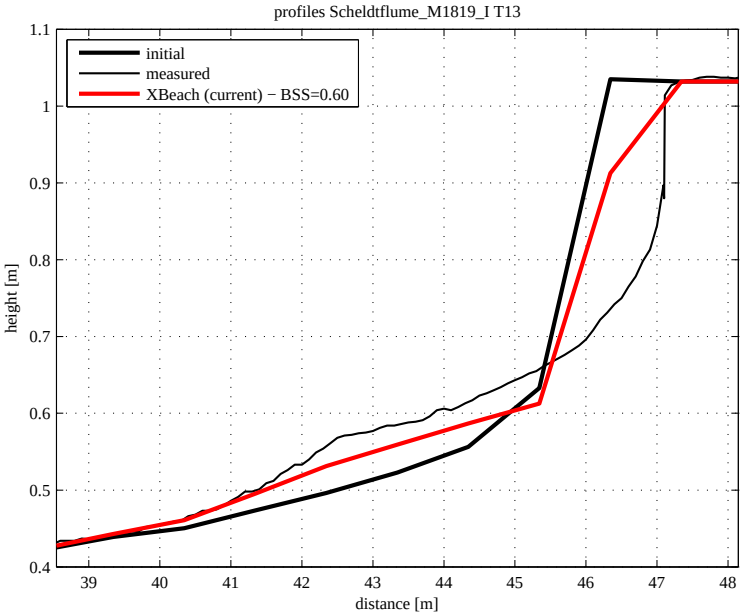

Figure 4.83: Final profile of test T13

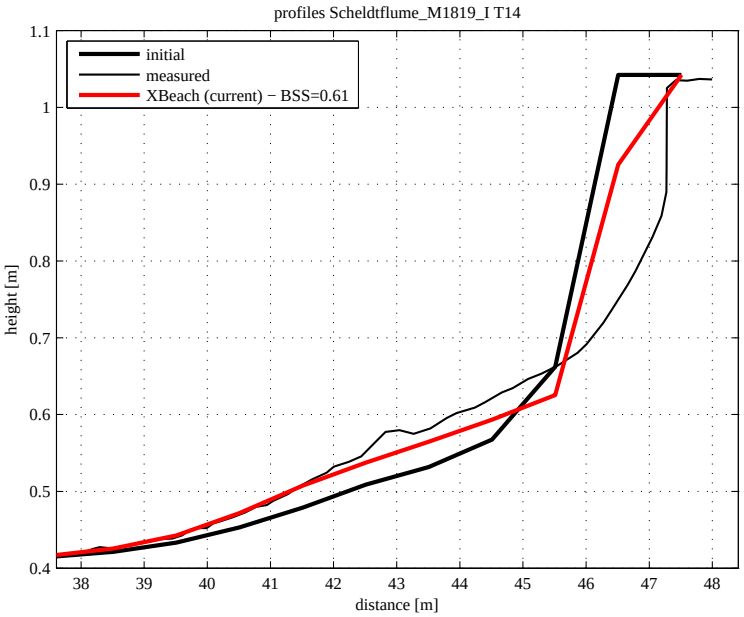

Figure 4.84: Final profile of test T14

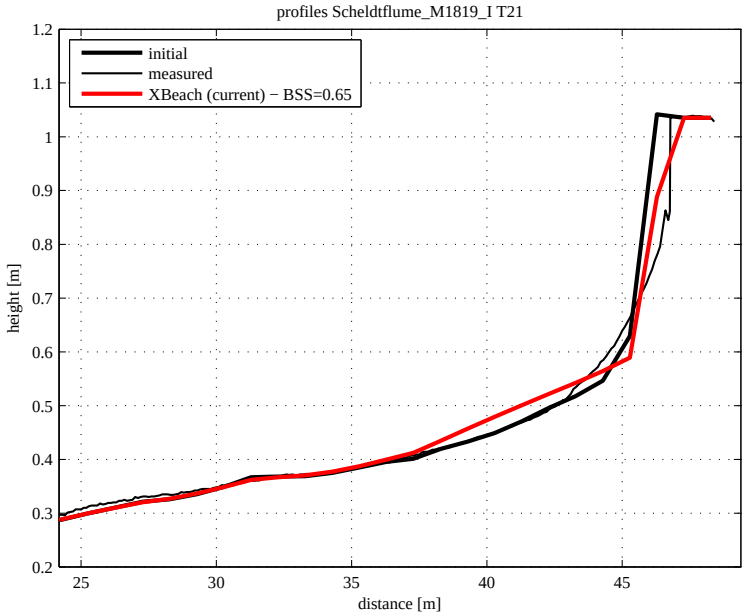

Figure 4.85: Final profile of test T21

These figures and tables are generated by the automated XBeach skillbed.
Something has gone wrong, so sadly no figure or table could be generated.

Figure 4.86: Final profile of test T22

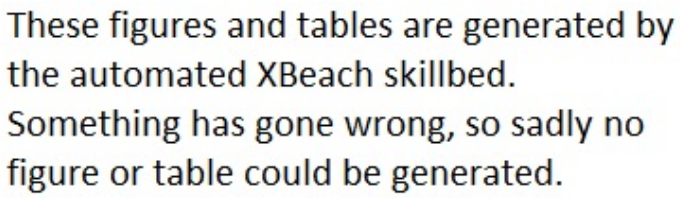

Figure 4.87: Final profile of test T23

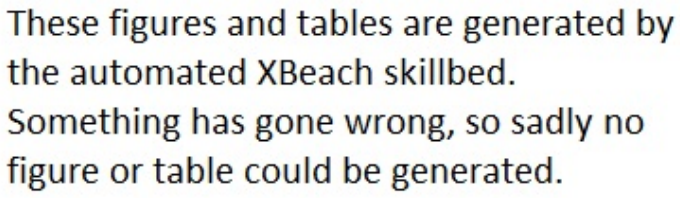

Figure 4.88: Final profile of test T24

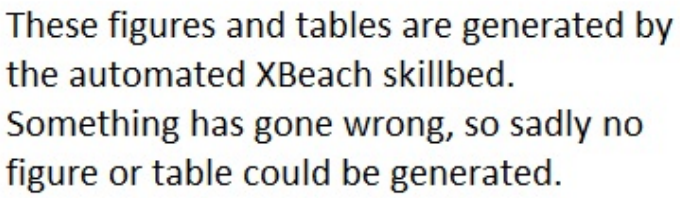

Figure 4.89: Final profile of test T25

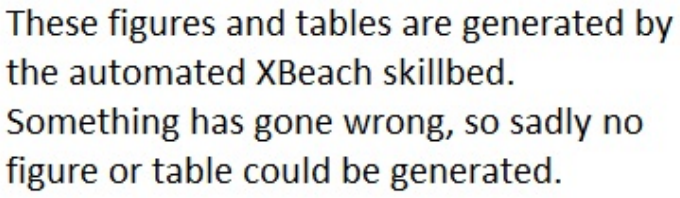

Figure 4.90: Final profile of test T26

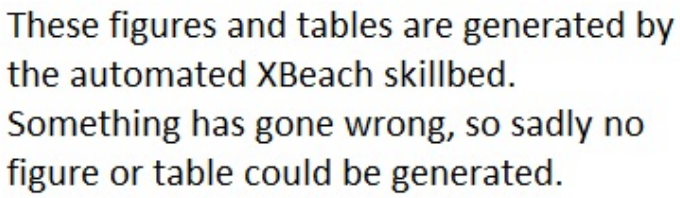

Figure 4.91: Final profile of test T27

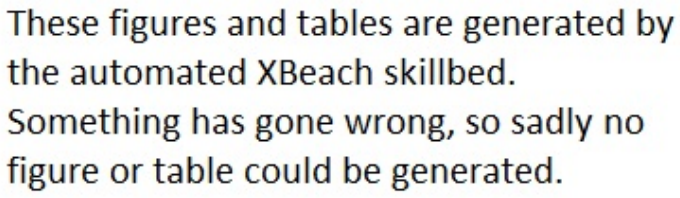

Figure 4.92: Final profile of test T28

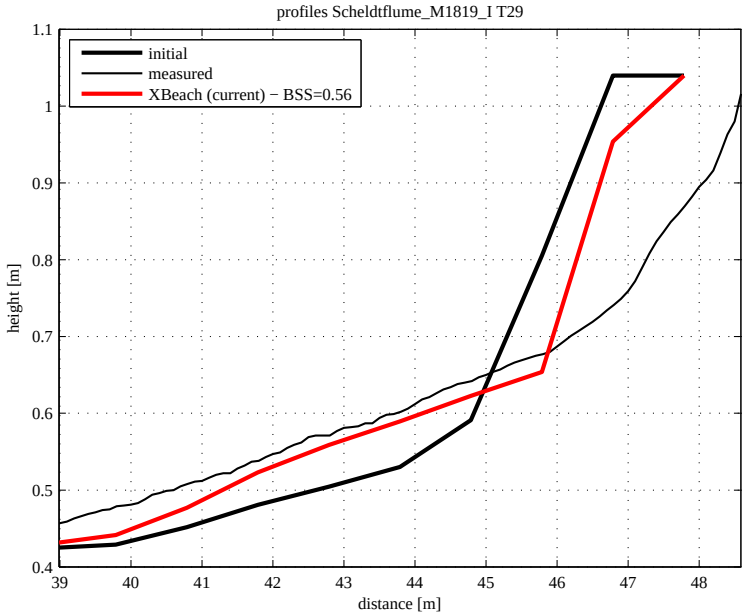

Figure 4.93: Final profile of test T29

4.2.4 H4265: Scheldt Flume 2003

During 2003, Scheldt Flume experiments were performed to assess the influence of the wave period on the amount of dune erosion. The tests are performed using a depth scale of 30, resulting in the profiles depicted in Figure 4.94 to Figure 4.100.

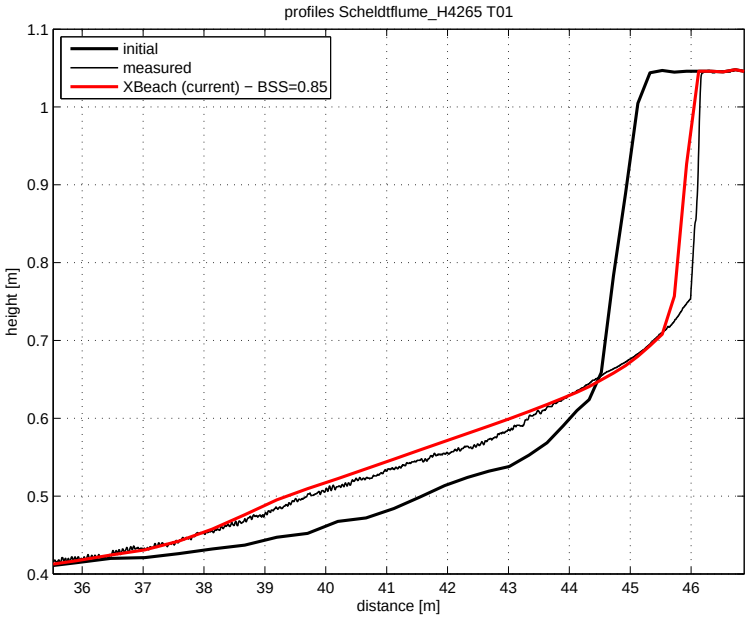

Figure 4.94: Final profile of test T01

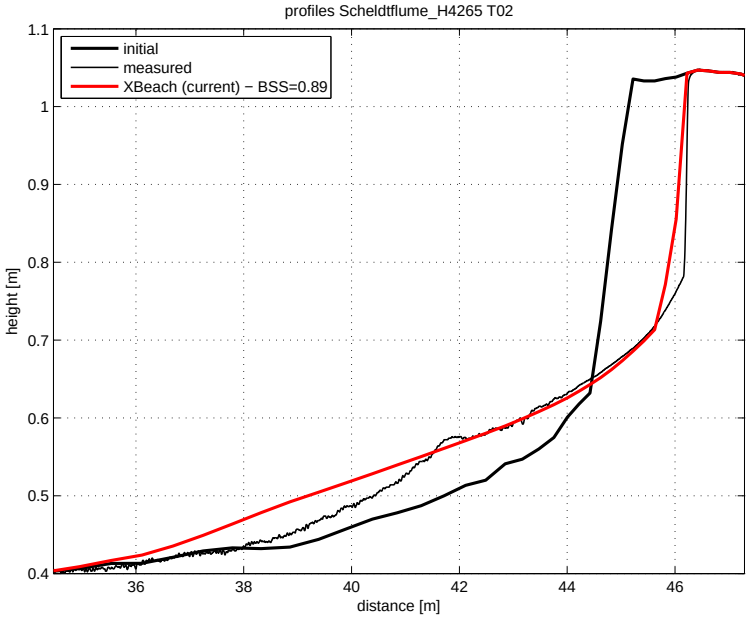

Figure 4.95: Final profile of test T02

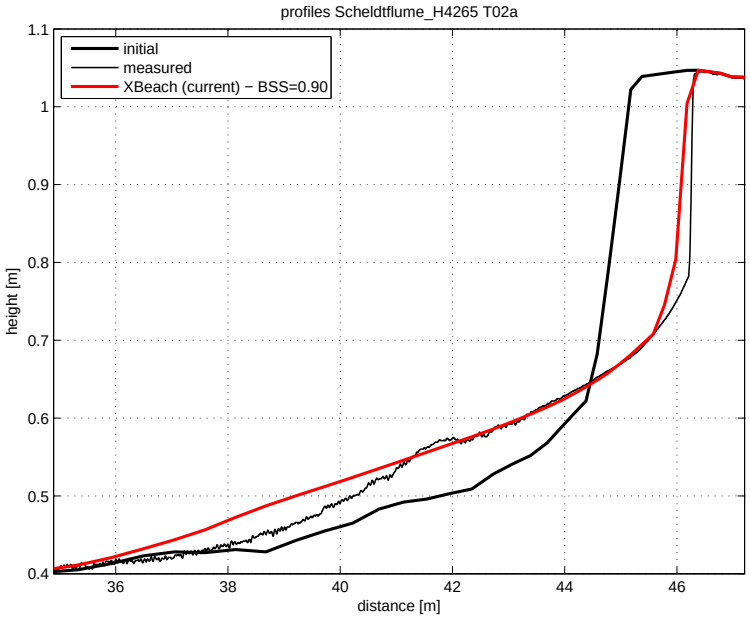

Figure 4.96: Final profile of test T02a

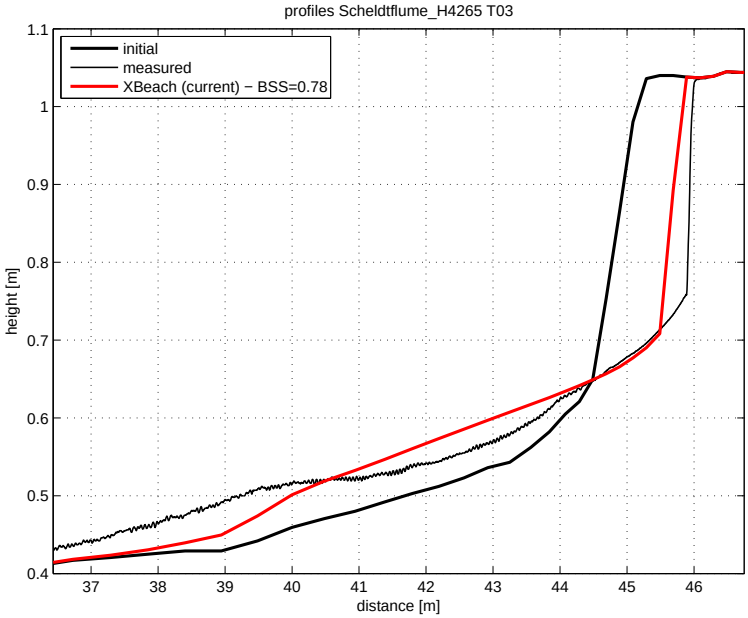

Figure 4.97: Final profile of test T03

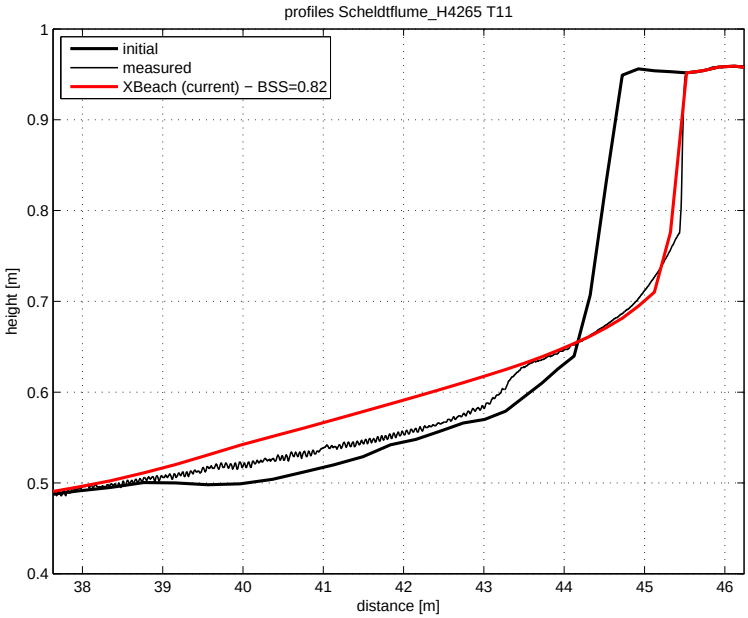

Figure 4.98: Final profile of test T011

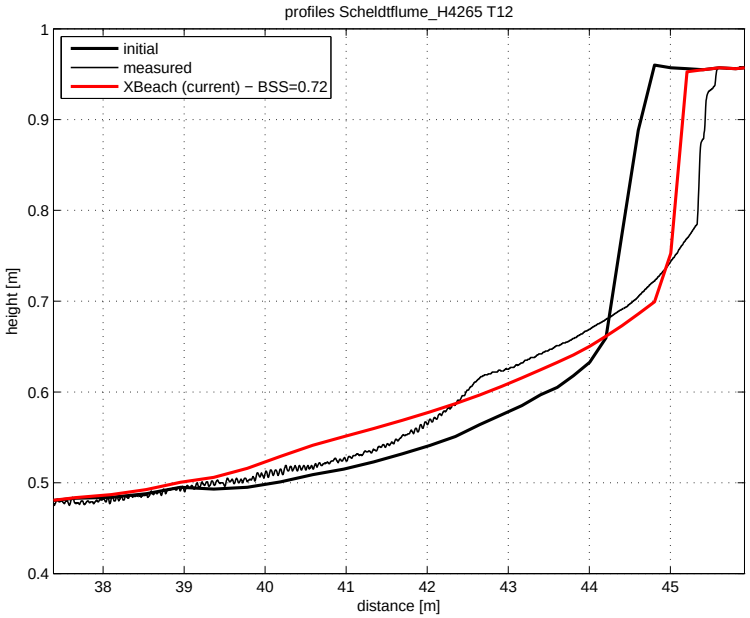

Figure 4.99: Final profile of test T012

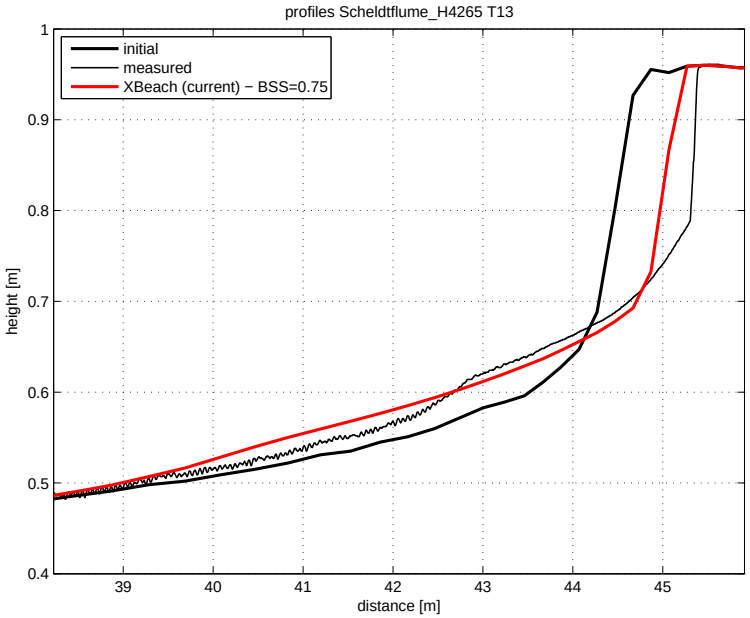

Figure 4.100: Final profile of test T013

4.3 Field measurements

4.3.1 1976 storm surge

In Figure 4.101, results of an XBeach simulation are compared to measurements from the storm surge that occurred on the night of January 2^{nd}, 1976.

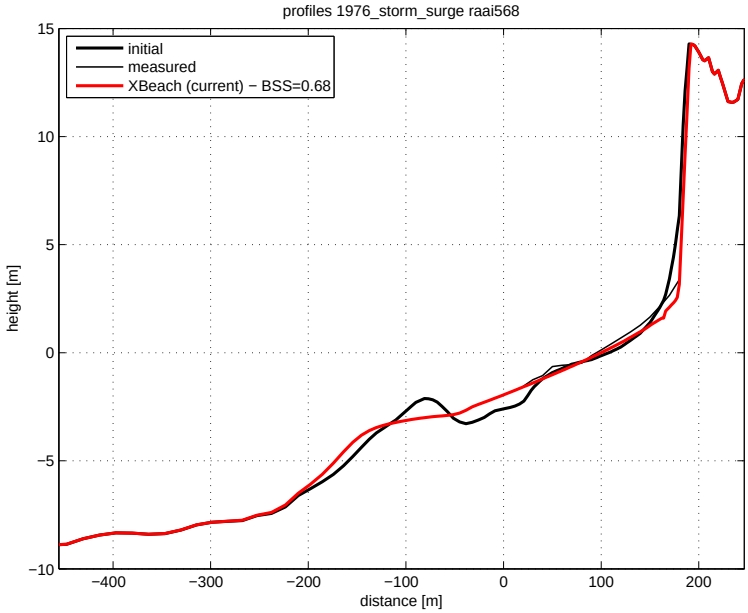

Figure 4.101: Final profile of raai 568

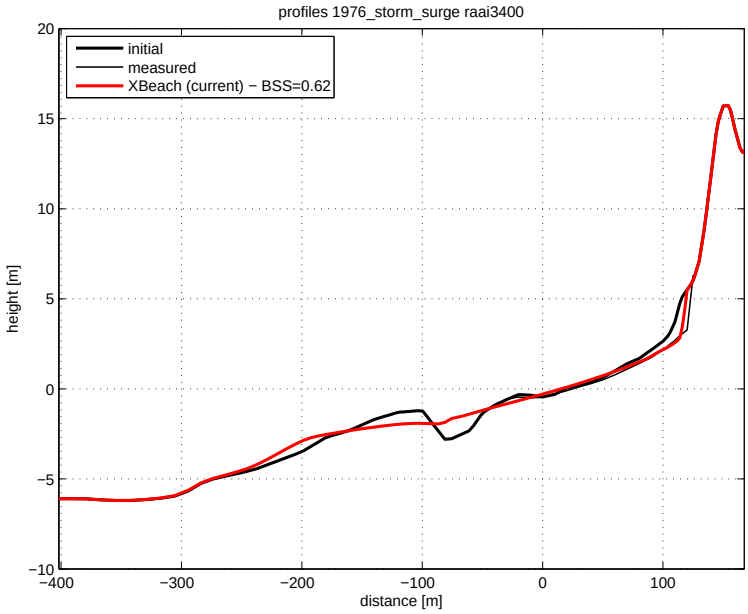

Figure 4.102: Final profile of raai 3400

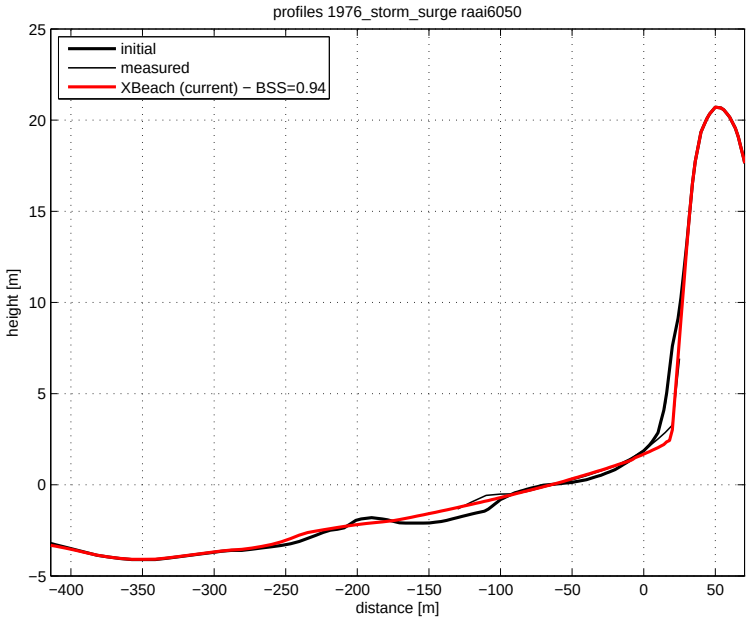

Figure 4.103: Final profile of raai 6050

Chapter 5

Scour and revetments

5.1 Small scale laboratory tests with revetments

5.1.1 M1819 III: Scheldt Flume 1981

The third part of the M1819 experiments contains several exploratory tests ($n_d = 15$) concerning dune revetments(Tilmans, 1983), the results of which are shown in Figure 5.1 to Figure 5.3.

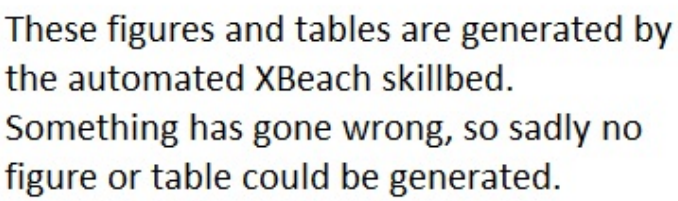

Figure 5.1: Final profile of test T02

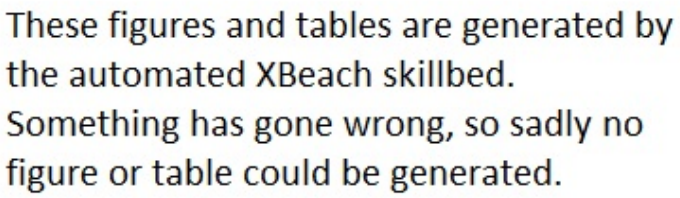

Figure 5.2: Final profile of test T03

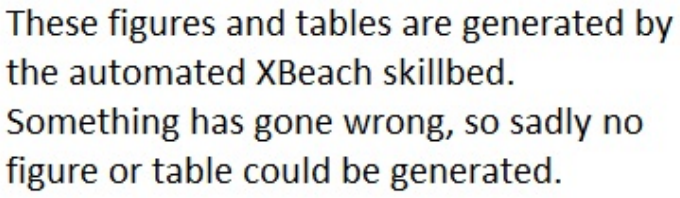

Figure 5.3: Final profile of test T04

5.2 Large scale laboratory tests with revetments

5.2.1 M1797: Deltaflume 1981

Figure 5.4 depicts the Schouwen profile from the M1797 test with dune revetment(Vellinga, 1981a).

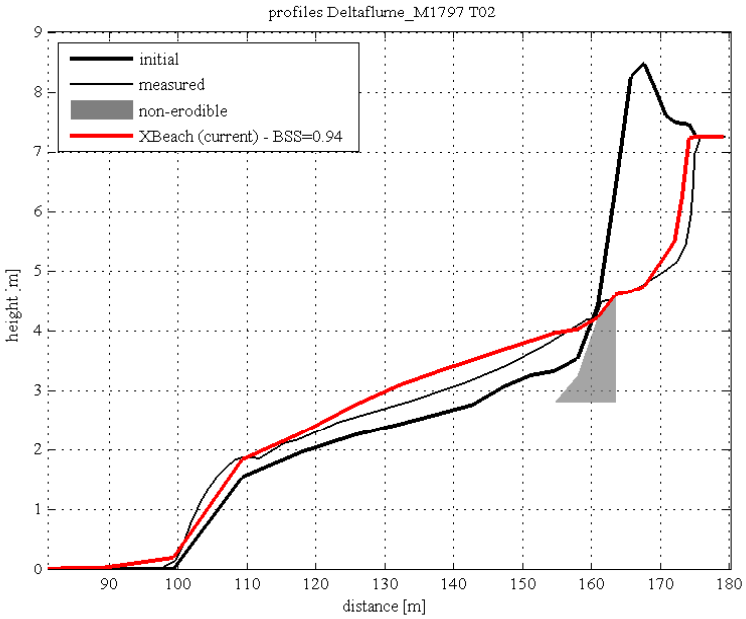

Figure 5.4: Final profile of test T02

5.2.2 H298: Deltaflume 1986

Steetzel (1987) describes a series of large scale experiments with revetments of different heights in the Delta Flume. A depthscale $n_d = 5$ is used for all experiments (Vellinga, 1986) and the initial profile in the flume correponds to the reference profile for the Holland coast. The location of the top of the revetment varied in each experiment, as can be seen in Figure 5.5 to Figure 5.7.

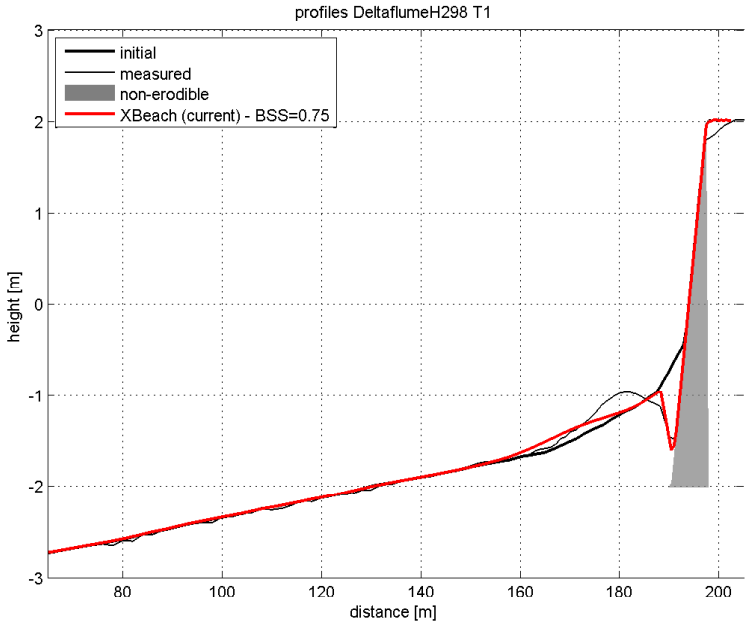

Figure 5.5: Final profile of test 1

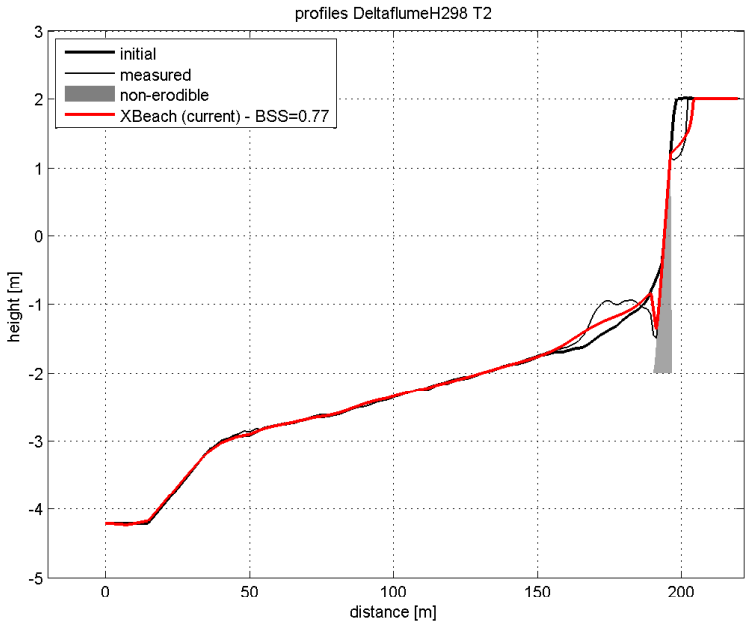

Figure 5.6: Final profile of test 2

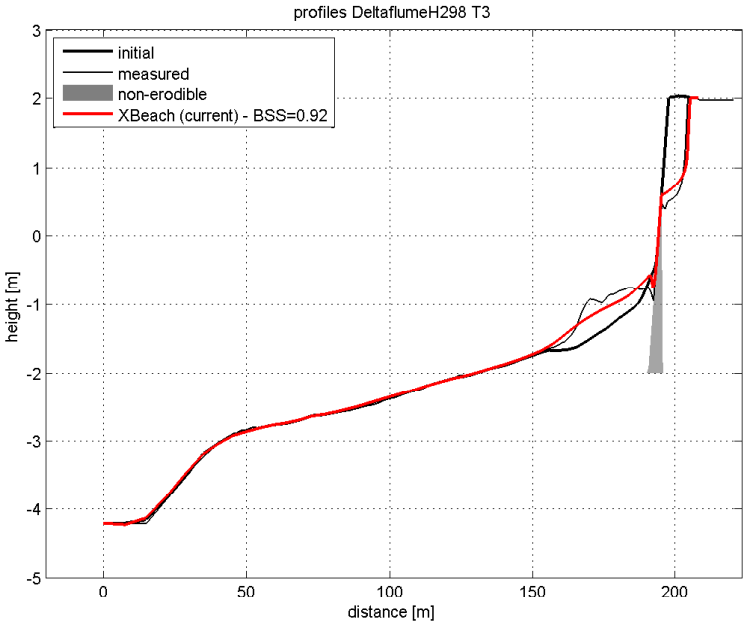

Figure 5.7: Final profile of test 3

5.2.3 H4731: Deltaflume 2006

In 2006, Delta Flume large scale experiments (depth scale of 6) were performed to gage the influence of collapsing dune revetments on dune erosion(Van Gent and Coeveld, 2007). Since XBeach can only handle solid structures, the collapse of the structure is not included in the simulations. Figure 5.8 to Figure 5.9 show the last measurement before the start of the collapse of the structure.

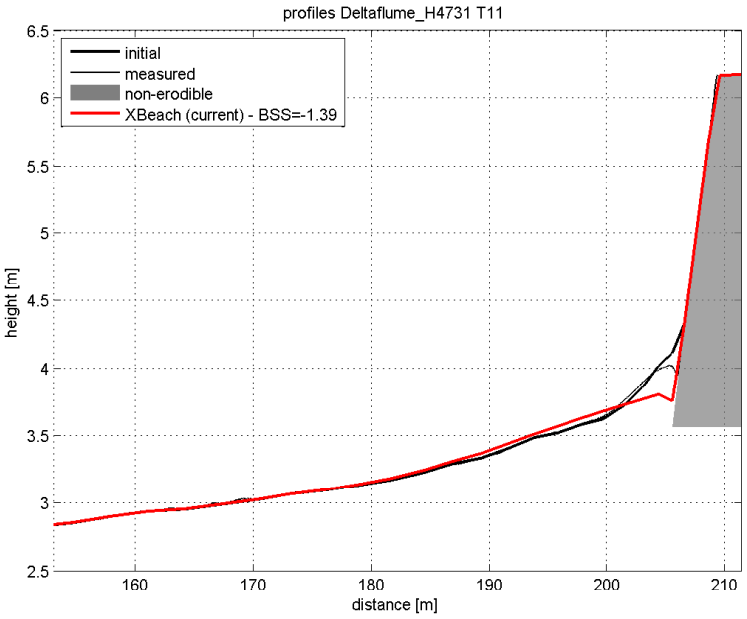

Figure 5.8: Final profile of test 11

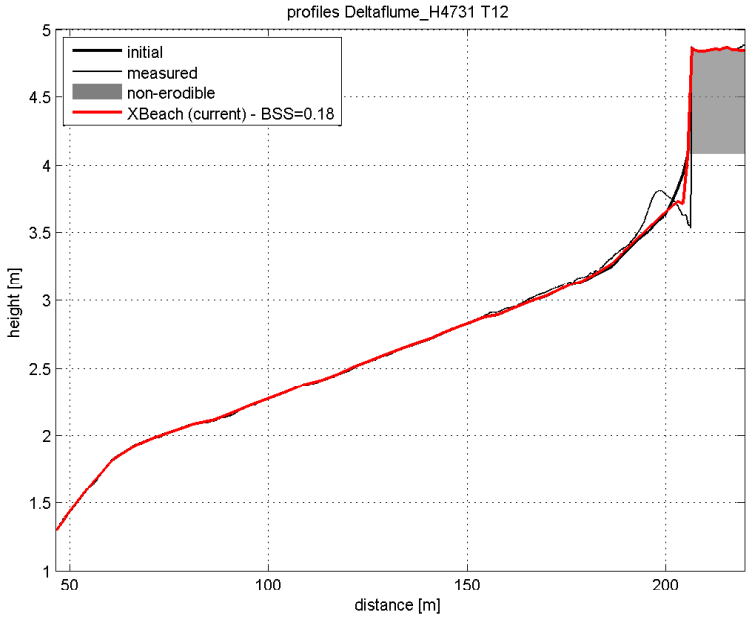

Figure 5.9: Final profile of test 12

Chapter 6

Model comparison

In this chapter, XBeach is compared to results obtained from other models. The comparisons are currently focused on the DUROS+ and D++ (Vellinga, 1986; Delft Hydraulics, 2006; Deltares, 2010) models that are used for the detailed assessment of dunes along the Dutch coast. Comparisons with other models like DurosTA (Steetzel, 1993) are made throughout the report and are not discussed specifically in this chapter.

6.1 Field applications

In this section, DUROS+ (Vellinga, 1986; Delft Hydraulics, 2006) and D++ are (Deltares, 2010) compared with XBeach based on field applications. Comparisons are made based on erosion volumes and retreat distances, since these are the main parameters of interest in dune safety assessment.

6.1.1 Retreat distances JARKUS

In this test, retreat distances obtained from DUROS+ and XBeach using a selection of JARKUS profiles characteristic for the Dutch coast are compared (Den Heijer et al., 2011). The comparison is presented in Figure 6.1. The retreat distance is defined as the horizontal distance between the NAP+5m contour and the erosion point. The erosion point is defined as the first diversion point between the pre-storm and post-storm profile, when going from the land side in seaward direction. Diversion is considered as a vertical difference of more than 5cm.

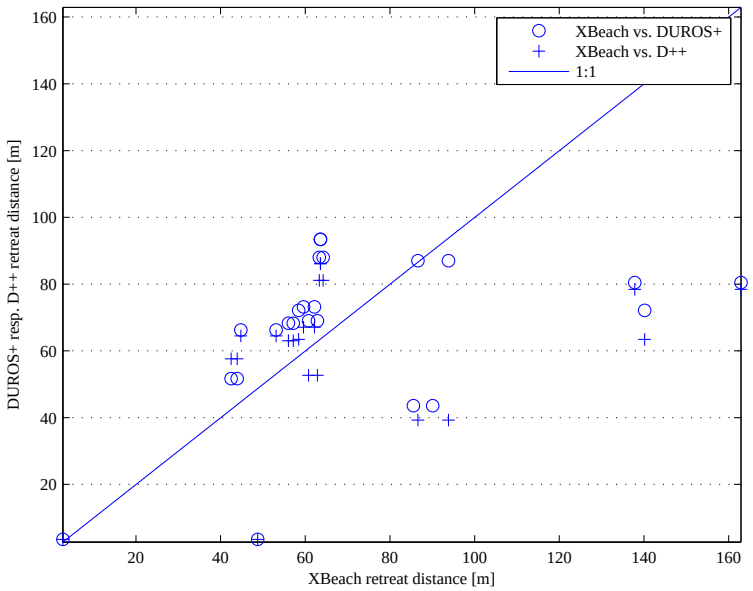

Figure 6.1: Scatter plot of retreat distances obtained from XBeach and DUROS+ (blue circle) and XBeach and D++ (green cross).

Chapter 7

References

Bakkenes, H. J. (2002). Observation and seperation of bound and free low-frequency waves in the nearshore zone. Master's thesis, Delft University of Technology.

Boers, M. (1996). Simulation of a surf zone with barred beach, part 1: Wave heights and wave breaking. Communications on Hydraulic and Geotechnical Engineering 69-5, Delft University of Technology. 116 p.

Carrier, G. F. and Greenspan, H. P. (1958). Water waves of finite amplitude on a sloping beach. *Journal of Fluid Mechanics*, 4:97–109.

Delft Hydraulics (2006). Dune erosion – product 2: Large-scale model tests and dune erosion prediction method. Report H4357, Delft Hydraulics.

Deltares (2010). Ontwikkeling detailtoets duinen 2011. Interim report 1202124-003, Deltares. in Dutch.

Den Heijer, C., Walstra, D. J. R., Van Thiel de Vries, J. S. M., Huisman, B. J. A., Hoonhout, B. M., Diermanse, F. L. M., and Van Gelder, P. H. A. J. M. (2011). Importance of dune erosion influencing processes. *Journal of Coastal Research*, SI 64(1):283–287. ISSN 0749-0208.

Murphy, A. H. and Epstein, E. S. (1989). Skill scores and correlation coefficients in model verification. *Monthly Whether Review*, 117:572–581.

Steetzel, H. J. (1987). Systematic research on the effectiveness of dune toe revetments - large scale model investigation. Technical Report H298-I, Delft Hydraulics.

Steetzel, H. J. (1993). *Cross-shore transport during storm surges*. PhD thesis, Delft University of Technology.

Sutherland, J., Peet, A. H., and Soulsby, R. L. (2004). Evaluating the performance of morphological models. *Coastal Engineering*, 51(8–9):917–939.

Tilmans, W. M. K. (1982). Systematic research of characteristic factors of dune erosion. Technical Report M1819 part I, Delft Hydraulics. in Dutch.

Tilmans, W. M. K. (1983). Exploratory research into the functioning of dune revetments during a super storm surge. Technical Report M1819 part III, Delft Hydraulics. in Dutch.

Van de Graaff, J. (1976). Scale series dune erosion. Technical Report M1263 part I, Delft Hydraulics. in Dutch.

Van Gent, M. R. A. and Coeveld, E. M. (2007). Influence of collapsed revetments on dune erosion. Technical Report H4731, Delft Hydraulics.

Van Gent, M. R. A., Van Thiel de Vries, J. S. M., Coeveld, E. M., De Vroeg, J. H., and Van de Graaff, J. (2008). Large-scale dune erosion tests to study the influence of wave periods. *Coastal Engineering*, 55(12).

Van Rijn, L. C., Walstra, D. J. R., Grasmeijer, B., Sutherland, J., Pan, S., and Sierra, J. P. (2003). The predictability of cross-shore bed evolution of sandy beaches at the time scale of storms and seasons using process-based profile models. *Coastal Engineering*, 47(3):295–327. ISSN 0378-3839.

Vellinga, P. (1981a). The functioning of dune revetments during a super storm surge. Technical Report M1797, Delft Hydraulics. in Dutch.

Vellinga, P. (1981b). Scale series dune erosion. Technical Report M1263 part II, Delft Hydraulics. in Dutch.

Vellinga, P. (1984). Scale series dune erosion: Large scale tests in deltaflume. Technical Report M1263 part III, Delft Hydraulics. in Dutch.

Vellinga, P. (1986). *Beach and Dune Erosion during Storm Surges*. PhD thesis, Delft University of Technology.

Appendix A

Model Performance Statistics

A.1 Introduction

In this Appendix the theory behind the Model Performance Statistics (MPS) used in the XBeach skillbed is explained. The MPS are used to quantify the performance of model results based on a comparison with measurement data. Different MPS parameters are used as each parameter has its own characteristics.

First an overview is given of the MPS parameters used in the XBeach skillbed, summarized in table form including some basic characteristics. Consequently, each MPS parameters listed in the overview table is further explained in separate sections.

A.2 MPS parameters

An overview of the MPS parameters used in the XBeach skillbed is given in Table A.1.

Table A.1: MPS parameters

Parameter	Description	Ranges
ME & STD	Mean Error & Standard Deviation	0: perfect prediction
R	Correlation coefficient (range: [0 1])	1: perfect correlation
Rel. bias	Systematic error relative to the mean	low value: good performance
Sci	Scatter Index	low values: performance
BSS	Brier Skill Score (Sutherland et al., 2004)	see below
BSS	Brier Skill Score (Murphy and Epstein, 1989)	see below

Each parameter listed in the table is further explained in the following paragraphs.

A.3 Mean Error & Standard Deviation

The Mean Error (ME) and the Standard Deviation (STD) of the error of a timeseries are a useful measure to quantify model performance for parameters such as wave heights or water levels. The SD is in general not so useful when applied to morphological parameters such as the bed leve evolution.

$$ME = \frac{1}{N}\sum_{i=1}^{N}(f_{comp.,i} - f_{meas.,i}) \tag{A.1}$$

$$STD = \sqrt{\frac{1}{N-1}\sum_{i=2}^{N}(f_{comp.,i} - f_{meas.,i} - ME)^2} \tag{A.2}$$

A.4 Correlation coefficient

The Correlation Coefficient R is a measure quantifying the correlation of the measurements and simulation results, but does not indicate significance because the distributions of the series are not taken into account.

A.5 Relative Bias

The Relative Bias (Rel. Bias) is the systematic error relative to the mean. Relative low values of the mean can cause high vales of the Rel. Bias.

$$Rel.Bias = \frac{\sum_{i=1}^{N}(f_{comp.,i} - f_{meas.,i})}{\sum_{i=1}^{N}\bar{f}_{meas.}} \tag{A.3}$$

A.6 Scatter Index

The Scatter index (Sci) is the standard deviation relative to the mean value of the measured signal. Relative low values of the mean can cause high vales of the Sci.

$$Sci = \frac{\sqrt{\frac{1}{N-1}\sum_{i=2}^{N}(f_{comp.,i} - f_{meas.,i} - ME)^2}}{\bar{f}_{meas.}} \tag{A.4}$$

A.7 Brier Skill Score

The Brier Skill Score (BSS) calculates the performance of the performance relative to a baseline prediction. The BSS calculates the mean square difference between the prediction

and observation with the mean square difference between baseline prediction and observation.

$$BSS = 1 - \frac{\frac{1}{N}\sum_{i=1}^{N}(z_{b,c} - z_{b,m})^2}{\frac{1}{N}\sum_{i=1}^{N}(z_{b,0} - z_{b,m})^2} \tag{A.5}$$

where $z_{b,c}$ is the computed bottom, $z_{b,m}$ is the measured bottom and $z_{b,0}$ is the initial bottom (variables taken at each cross-shore coordinate i).

Perfect agreement gives a Brier score of 1, whereas modelling the baseline condition gives a score of 0. If the model prediction is further away from the final measured condition than the baseline prediction, the skill score is negative. Van Rijn et al. (2003) proposed a classification for the Brier Skill Score as shown in Table A.2.

The BSS is very suitable for the prediction of bed evolution. The baseline prediction for morphodynamic modelling will usually be that the initial bed remains unaltered. In other words, the initial bathymetry is used as the baseline prediction for the final bathymetry. A limitation of the BSS is that it cannot account for the migration direction of a bar; it just evaluates whether the computed bed level (at time t) is closer to the measured bed level (at time t) than the initial bed level. If the computed bar migration is in the wrong direction, but relatively small; this may result in a higher BSS compared to the situation with bar migration in the right direction, but much too large. The BSS will even be negative, if the bed profile in the latter situation is further away from the measured profile than the initial profile. The limitation shown here is that position and amplitude errors are included in the BSS. Distinguishing position errors from amplitude errors, requires a visual inspection of measured and modelled profiles or the calculation of further statistics (Murphy and Epstein, 1989). The BSS can be extremely sensitive to small changes when the denominator is low, in common with other non-dimensional skill scores derived from the ratio of two numbers.

Table A.2: Brier Skill Score quantification (Van Rijn et al., 2003)

Qualification	Brier Skill Score
Excellent	1.0 - 0.8
Good	0.8 - 0.6
Reasonable fair	0.6 - 0.3
Poor	0.3 - 0.0
Bad	<0.0

A.8 Brier Skill Score (Murphy and Epstein, 1989)

Murphy and Epstein (1989) decomposed the BSS, leading to contributions due to errors in predicting the amplitude (α), the phase (β) and the mean (γ) as presented in Table A.3. The decomposition facilitates linking performance quantifications to model processes and accordingly bringing the model performance to a higher level.

$$BSS = \frac{\alpha - \beta - \gamma + \epsilon}{1 + \epsilon} \tag{A.6}$$

$$\alpha = r^2_{Y'X'}; \beta = (r_{Y'X'} - \frac{\sigma_{Y'}}{\sigma_{X'}})^2; \gamma = (\frac{<Y'> - <X'>}{\sigma_{X'}})^2; \epsilon = \frac{<X'>^2}{\sigma_{X'}} \tag{A.7}$$

Table A.3: Brier Skill Score decomposition factors (Murphy and Epstein, 1989)

Factor	Indication	Perfect modelling
phase error (α)	transport locations	$\alpha = 1$
amplitude error (β)	transport volumes	$\beta = 0$
map mean error (γ)	-	$\gamma = 0$
normalization term (ϵ)	-	-

Van Rijn et al. (2003) also proposed a classification for the decomposed Brier Skill Score as shown in Table A.4.

Table A.4: Brier Skill Score (Murphy and Epstein, 1989) quantification (Van Rijn et al., 2003)

Qualification	Brier Skill Score
Excellent	1.0 - 0.5
Good	0.5 - 0.2
Reasonable fair	0.2 - 0.1
Poor	0.1 - 0.0
Bad	<0.0